Large-scale correlated calculations of linear optical absorption and low-lying excited states of polyacenes: Pariser-Parr-Pople Hamiltonian

Priya Sony* and Alok Shukla†
Physics Department, Indian Institute of Technology, Powai, Mumbai 400076, India
(Received 12 July 2006; revised manuscript received 7 December 2006; published 27 April 2007)

We present large-scale correlated calculations of the linear optical absorption spectrum of oligo-acenes containing up to seven benzene rings. For the calculations we used the Pariser-Parr-Pople (PPP) Hamiltonian, along with the configuration interaction (CI) technique at various levels such as the full CI, the quadruple CI, and multireference singles-doubles CI. The role of Coulomb parameters used in the PPP Hamiltonian was examined by considering standard Ohno parameters, as well as a screened set of parameters. A detailed analysis of the many-body character of the important excited states contributing to the linear absorption has also been performed. The results of our calculations have been compared extensively with the theoretical work of other authors, as well as with experiments.

DOI: 10.1103/PhysRevB.75.155208 PACS number(s): 78.30.Jw, 78.20.Bh, 42.65.−k

I. INTRODUCTION

In last few decades, there has been intensive research in the field of the optical properties of acenes.[1–5] It is well known that with the increase in the number of benzene rings in the acenes, the highest occupied molecular orbital (HOMO) to lowest unoccupied molecular orbital (LUMO) gap decreases, making the material more conducting. It is in fact believed that an infinite linear acene—i.e., the polyacene—could be a metal[4] and, at low temperatures, a superconductor.[5] Thus, higher acenes can prove to be potential candidates for preparing both optical and electronic devices. Polyacenes generally crystallize in well-defined structures, and their crystalline forms have found applications in novel opto-electronic devices such as light-emitting field-effect transistors.[6] Three-dimensional structures of polyacenes have also been investigated theoretically for their electronic structure, transport, and optical properties by several authors.[7–9] Oligomers of polyacene such as naphthalene, anthracene, tetracene, pentacene, etc., are materials which are well known for their interesting optical properties.[10] Because of the high symmetry, they have separate optical responses to radiation polarized along the conjugation direction, in relation to the radiation polarized perpendicular to it. Several experimental investigations of the linear optical properties of polyacenes have been performed over the years. These include linear-absorption-based studies of naphthalene,[11–19] anthracene,[11,12,14,20–28] tetracene,[11,12,29–34] pentacene,[11,12,29,34–41] and hexacene.[12,42] Several theoretical studies of the low-lying excited states of these materials have also been performed, such as the early linear-combination-of-atomic-orbitals- (LCAO-) based study by Coulson,[43] LCAO-MO and perimeter MO approach by Pariser,[44] a free-electron-gas approach by Platt[45] and Ham and Ruedenberg,[46] complete neglect of differential overlap (2) configuration interaction (CNDO/2 CI) approach by Hofer and Hedges,[47] *ab initio* multireference Møller-Plesset (MRMP) theory,[48] density-matrix renormalization-group (DMRG) theory using the Pariser-Parr-Pople (PPP) model Hamiltonian,[49,50] *ab initio* density-functional-theory- (DFT-) based methodologies,[8,51–55] self-consistent field-random phase approximation (SCF-RPA) scheme using the PPP model Hamiltonian,[56] and CNDO/S2 model parametrization technique by Lipari and Duke[57] Among the more recent studies using the PPP model Hamiltonian and many-body methodologies, those of Raghu and co-workers[49,50] are the foremost.

Most of the theoretical studies mentioned above either concentrate on a class of excited states of polyacenes or restrict themselves to the study of smaller oligomers. In some earlier studies, chiefly because of the lack of computer power at the time, the level of treatment of electron-correlation effects was rather modest by contemporary standards. Additionally, to the best of our knowledge, none of the earlier theoretical studies reported calculations of the optical absorption spectrum of these materials. Therefore, we believe that there is a need to perform systematic large-scale many-body calculations of the optical properties of these materials with the following aims in mind: (i) to compute the linear optical absorption spectra of a range of oligoacenes, (ii) to understand their evolution with increasing size of the oligomers, (iii) to understand the influence of electron correlation effects on them, and finally (iv) to understand the nature of low-lying excited states contributing to the linear optics. As is well known, in quasi-one-dimensional materials such as conjugated polymers, electron-correlation effects have a profound influence on their optical properties.[58] It is with all these issues in mind, in the present work, in a systematic manner, that we undertake a large-scale correlated study of linear optical absorption in oligoacenes of increasing sizes—namely, from naphthalene to heptacene. The optical absorption spectra have been computed for both the radiation polarized along the conjugation direction and the one polarized perpendicular to it. We have used the PPP Hamiltonian for the purpose and utilized various CI techniques such as the full CI (FCI), the quadruple CI (QCI), and the multireference singles-doubles CI (MRSDCI) methods. The CI-based correlation methodology used in the present work is sound and has been used successfully by us in the past to study the linear and nonlinear optical properties of various other conjugated polymers.[59–64] Additionally, we have also examined the issue of the influence of Coulomb parameters on the results by performing calculations with two distinct sets of

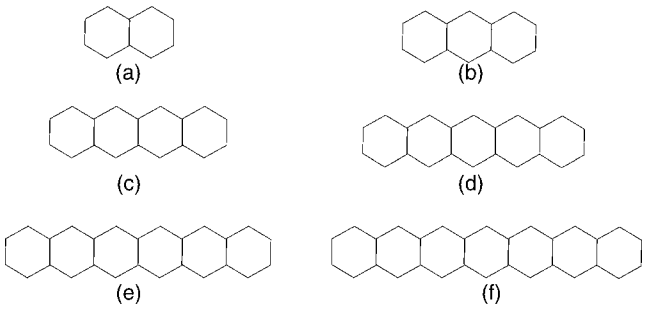

FIG. 1. Schematic drawings of polyacenes considered in this work—namely, (a) naphthalene, (b) anthracene, (c) tetracene, (d) pentacene, (e) hexacene, and (f) heptacene

parameters—namely, the standard Ohno parameters[65] and a screened set of parameters meant for phenylene-based conjugated polymers[66]—to describe the P-P-P model Hamiltonian.

The remainder of this paper is organized as follows. In Sec. II we briefly review the theoretical methodology adopted in this work. In Sec. III we present and discuss our results of the optical absorption spectra of various oligoacenes. Finally, in Sec. IV we summarize our conclusions and present possible directions for future research work.

II. THEORY

The structures of oligoacenes ($C_{4n+2}H_{2n+4}$, $n=2$, 3, 4, 5, 6, and 7) starting from naphthalene up to heptacene are shown in Fig. 1. Oligomers were assumed to lie in the xy plane with the conjugation direction taken to be along the x axis. They can be seen as a series of benzene rings fused together, along the conjugation direction. An alternative way to look at the structure of oligoacenes is to visualize them as two vertically displaced polyene chains coupled with each other along the y axis via hopping and the Coulomb interactions. From this viewpoint, polyacene is a ladderlike polymer. The point group symmetry of oligoacenes is D_{2h}, so that the one-photon states belong to the irreducible representations (irreps) B_{3u} or B_{2u}, while the ground state belongs to the irrep A_g. Also, by convention we assign the ground state a negative $(-)$ particle-hole symmetry. Therefore, by dipole selection rules, all the optically allowed states must have positive $(+)$ particle-hole symmetry. Thus, the states with negative particle-hole symmetry will not be visible in the linear optical spectrum. However, we have calculated the energy of the $1B_{3u}^-$ state, together with the optically allowed $1B_{2u}^+$ and $1B_{3u}^+$ states, for the sake of comparison with the experimental and other theoretical results. Clar classified the absorption spectra into three bands—namely, p, α, and β.[10] In our work, the transition to the $1B_{2u}^+$ state from the $1A_g^-$ ground state via a short-axis (y-axis) polarized photon corresponds to the p band (^1L_a band of Platt[45]). Similarly, the transition from the ground state to $1B_{3u}^-$ and $1B_{3u}^+$ via a long-axis (x-axis) polarized photon corresponds to the α (^1L_b band of Platt[45]) and the β (^1B_b band of Platt[45]) bands, respectively.

The correlated calculations on the oligoacenes were performed using the PPP model Hamiltonian, which can be written as

$$H = H_{C_1} + H_{C_2} + H_{C_1C_2} + H_{ee}, \tag{1}$$

where H_{C_1} and H_{C_2} are the one-electron Hamiltonians for the carbon atoms located on the upper and lower polyene chains, respectively. $H_{C_1C_2}$ is the one-electron hopping between the two chains, and H_{ee} depicts the electron-electron repulsion. The individual terms can now be written as

$$H_{C_1} = -t_0 \sum_{\langle k,k' \rangle} B_{k,k'}, \tag{2a}$$

$$H_{C_2} = -t_0 \sum_{\langle \mu,\nu \rangle} B_{\mu,\nu}, \tag{2b}$$

and

$$H_{C_1C_2} = -t_\perp \sum_{\langle k,\mu \rangle} B_{k,\mu}, \tag{2c}$$

$$H_{ee} = U \sum_i n_{i\uparrow} n_{i\downarrow} + \frac{1}{2} \sum_{i \neq j} V_{i,j} (n_i - 1)(n_j - 1). \tag{3}$$

In the equation above, k and k' are carbon atoms on the upper polyene chain, and μ and ν are carbon atoms located on the lower polyene chain, while i and j represent all the atoms of the oligomer. The symbol $\langle \cdots \rangle$ implies nearest neighbors, and $B_{i,j} = \Sigma_\sigma (c_{i,\sigma}^\dagger c_{j,\sigma} + \text{H.c.})$. The matrix elements t_0 and $t_\perp$ depict one-electron hops. As far as the values of the hopping matrix elements are concerned, we took $t_0 = 2.4$ eV for both intracell and intercell hopping, and $t_\perp = t_0$, consistent with the undimerized ground state for polyacene argued by Raghu *et al.*[49] Consequently, the carbon-carbon bond length has been fixed at 1.4 Å, and all bond angles have been taken to be 120°. At this point it is worthwhile to discuss the issue of the ground-state geometry of oligoacenes. Experimentally speaking, to the best of our knowledge, the available data on the ground-state geometry of various polyacenes are for the crystalline phase.[67] Therefore, as far as the ground-state geometries of isolated chains are concerned, theoretical calculations based upon geometry optimization provide very important input. However, the picture which emerges from such calculations is far from clear. Raghu *et al.*[49] studied the ground-state geometry of polyacenes using a DMRG-based approach and concluded that the Peierls' instability in this polymer is conditional, with the gain in the electronic energy being proportional to δ^2 (δ is the dimerization amplitude), rather than δ which is the case for *trans*-polyacetylene. In their next paper, Raghu *et al.*[50] concluded that the ground-state geometry of polyacene consists of a weakly distorted structure with undimerized chains, coupled by slightly longer rungs. Therefore, Raghu *et al.*[50] used an undistorted geometry in their excited-state calculations. Houk *et al.*,[55] based upon their *ab initio* DFT-based calculations, had also predicted a ground state similar to that of Raghu *et al.*[50] Several workers have suggested that due to Peierls distortion acenes possess nonsymmetric geometry,[51,53,68,69] but on the other hand Cioslowski[70] has reported that at the correlated level, the symmetric geometry is more stable. Also, Garcia-Bach and co-workers[71] studied the distortion of polyacenes within a many-body valence-bond framework and have suggested

that all the structures (symmetric or nonsymmetric) are close in energy with the symmetric one possessing the lowest energy. Moreover, Niehaus *et al.*[72] have recently studied polyacenes using a tight-binding-based Green's-function approach and reported that for $n \leqslant 19$ the symmetric structure is the most stable. Therefore, keeping these uncertainties in mind and the fact that our main aim is to study the influence of electron correlations on the optical properties of oligoacenes, we have performed our calculations using the symmetrical structure for oligoacenes. This choice also allows us to compare our results directly with those of Ramasesha and co-workers,[50,73,74] who also employed a symmetric geometry in their excited state of oligoacenes using the PPP model Hamiltonian.

The Coulomb interactions are parametrized according to the Ohno relationship[65]

$$V_{i,j} = U/\kappa_{i,j}(1 + 0.6117R_{i,j}^2)^{1/2}, \tag{4}$$

where $\kappa_{i,j}$ depicts the dielectric constant of the system which can simulate the effects of screening, U is the on-site repulsion term, and $R_{i,j}$ is the distance in Å between the ith carbon and the jth carbon. In the present work, we have performed calculations with two parameter sets: (a) "standard parameters" with $U=11.13$ eV and $\kappa_{i,j}=1.0$ and (b) "screened parameters" with $U=8.0$ eV and $\kappa_{i,j}=2.0$ $(i \neq j)$ and $\kappa_{i,i}=1$, proposed initially by Chandross and Mazumdar to study phenyl-based conjugated polymers.[66] In our earlier studies of phenyl-based conjugated polymers such as the PDPA, PPP, PPV, etc., we found that the screened parameters generally provided a much better description of their optical properties as compared to the standard ones.[59–64]

The starting point of the correlated calculations for various oligomers were restricted Hartree-Fock (HF) calculations, using the PPP Hamiltonian. The many-body effects beyond the HF calculations were computed using different levels of the CI method—namely, FCI, QCI, and MRSDCI. Details of these CI-based many-body procedures have been presented in our earlier works.[59,60,62,63] From the CI calculations, we obtain the eigenfunctions and eigenvalues corresponding to the correlated ground and excited states of various oligomers. The many-body wave functions are used to compute the matrix elements of the dipole operator connecting the ground state to various excited states. These dipole matrix elements are in turn used to calculate the linear optical absorption spectra of various polyacenes.

III. CALCULATIONS AND RESULTS

In this section, first we will briefly discuss the main features of the linear optical spectra of polyacenes computed within the independent-electron Hückel model. Next we will present and discuss the main results of this work—namely, the correlated linear absorption spectra of oligoacenes of increasing sizes—and compare our results with the other available experimental and theoretical results. A preliminary description of the results for tetracene and pentacene was presented in an earlier work.[75] However, the results presented here are based upon more extensive calculations, and, therefore, they supersede our earlier results.[75]

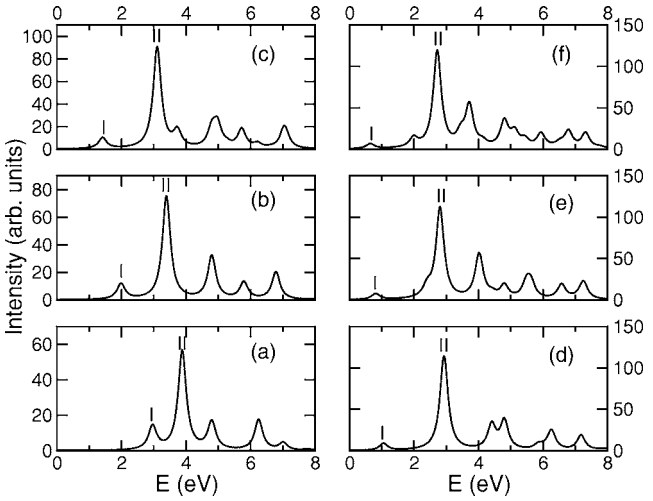

FIG. 2. Linear optical absorption spectra of (a) naphthalene, (b) anthracene, (c) tetracene, (d) pentacene, (e) hexacene, and (f) heptacene. In all cases a linewidth of 0.15 eV was assumed.

A. Hückel model results

Here we briefly discuss the salient features of the linear absorption spectra of oligoacenes computed using the tight-binding Hückel model and presented in Fig. 2.

For all the oligomers, the first peak (labeled I) corresponds to π-π^* excitation described by the HOMO (H) $\rightarrow$LUMO (L) transition through a y-polarized photon leading to the $1B_{2u}^+$ excited state of the system. However, with the increasing size of the oligomer, the intensity of this $H \rightarrow L$ transition decreases, which is understandable because, in the thermodynamic limit, with the chosen hopping parameters, the polyacene is metallic. The highest-intensity peak (labeled II) for each of the oligoacenes investigated corresponds to an x-polarized photon leading the system to its $1B_{3u}^+$ excited state. For oligomers with n=even, the highest-intensity peak corresponds to the transitions $H \rightarrow L+n/2$ and $H-n/2 \rightarrow L$, while for those with n=odd, the peak II corresponds to the transitions $H \rightarrow L+(n\pm1)/2$ and $H-(n\pm1)/2 \rightarrow L$. Moreover, as the lengths of the oligoacenes increase, as expected, the spectrum is redshifted due to delocalization of the particle-hole pair.

B. PPP calculations

Here we present the results of our correlated calculations of linear absorption on oligoacenes using the PPP model Hamiltonian. First we present and discuss our results for individual acenes, followed by a unified discussion of their spectra. In Table I we present the number of reference states (N_{ref}) and the dimension of the Hamiltonian matrix (N_{total}) used in our CI calculations for different symmetry subspaces of various oligomers. The fact that the calculations presented here are quite large scale is obvious from N_{total}, which, e.g., for pentacene was in excess of 1×10^6 for the A_g and B_{2u} symmetries. Therefore, we are confident that our results take into account the influence of electron-correlation effects quite accurately.

TABLE I. The number of reference configurations (N_{ref}) and the total number of configurations (N_{total}) involved in the MRSDCI (or FCI or QCI, where indicated) calculations for different symmetry subspaces of various oligoacenes.

	A_g		B_{2u}		B_{3u}	
Oligomer	N_{ref}	N_{total}	N_{ref}	N_{total}	N_{ref}	N_{total}
Naphthalene	1[a]	4936[a]	1[a]	4794[a]	1[a]	4816[a]
Anthracene	1[a]	623576[a]	1[a]	618478[a]	1[a]	620928[a]
Tetracene	1[b]	193538[b]	1[b]	335325[b]	24[c,d]	34788[c,d]
Pentacene	1[b]	1002597[b]	1[b]	1707243[b]	38[c]	130196[c]
					34[d]	126690[d]
Hexacene	66[c]	460527[c]	28[c]	191944[c]	54[c]	393248[c]
	40[d]	299141[d]	32[d]	242013[d]	30[d]	252420[d]
Heptacene	45[c]	590599[c]	30[c]	415999[c]	40[c,d]	653476[c,d]
	36[d]	480032[d]	22[d]	270391[d]		

[a]FCI method with standard as well as screened parameters.
[b]QCI method with standard as well as screened parameters.
[c]Using standard parameters.
[d]Using screened parameters.

Before discussing the individual oligomers, we would like to summarize the patterns that emerge from the computed optical absorption spectra of acenes ranging from naphthalene to heptacene. The absorption spectrum of all the oligoacenes, irrespective of the PPP parameters used in the calculations, contains the following important features.

(i) The first peak in the absorption spectrum for all the oligomers studied corresponds to the $1B_{2u}^{+}$ excited state of the system. The most important configuration contributing to the many-particle wave function of the state corresponds to the $|H \rightarrow L\rangle$ excitation, in agreement with Hückel model calculations. The relative intensity of this feature decreases with the increasing size of the oligomer, again in agreement with the Hückel model results.

(ii) The second and the most intense feature in the spectrum corresponds to the $1B_{3u}^{+}$ state, obtained by the absorption of an x-polarized photon. The most important configurations contributing to the wave function of this state, for n =even oligomers, are excitations $|H \rightarrow L+n/2\rangle$ and $|H-n/2 \rightarrow L\rangle$ and, for n=odd, the excitations $|H \rightarrow L+(n\pm1)/2\rangle$ and $|H-(n\pm1)/2 \rightarrow L\rangle$. This aspect of the correlated spectrum is also in good agreement with the Hückel model results.

(iii) Another important state—namely, the $1B_{3u}^{-}$ state—exists for all oligoacenes. Because it has the same particle-hole symmetry $(-)$ as the ground state, in PPP (and Hückel) calculations it does not contribute to the absorption spectrum. But many experiments report this state as a very weak feature in the absorption spectrum. In our calculations, for naphthalene and anthracene, this state occurs at energies lower than the $1B_{2u}^{+}$ state, but for longer oligomers, it is at higher excitation energies than the $1B_{2u}^{+}$ state. The important configurations contributing to the wave function of this state are the same as the ones contributing to $1B_{3u}^{+}$, except for their opposite relative signs, for all the oligomers up to pentacene. But from hexacene onwards, it is the doubly excited configurations that contribute significantly to this state. Thus, it is the electron-correlation effects which are responsible for its distinct location in the spectrum as compared to the $1B_{3u}^{+}$ state.

(iv) Generally, the spectra computed with the standard parameters are in good qualitative agreement with those computed with the screened parameters. Quantitatively speaking, screened parameter spectra are redshifted as compared to the standard parameter ones and are in better agreement with the experiments for longer acenes.

(v) Although there are some qualitative similarities between the PPP and Hückel model results, quantitatively speaking the optical gaps obtained using the Hückel model are much smaller than their PPP and experimental counterparts.

Having emphasized the general features of our work, next we discuss the results of our calculations for individual oligomers and compare them with the theoretical results of other authors and the experimental ones. Quantitative aspects of our calculations are summarized in Table II, which also reports some of the experimental and the theoretical results of other authors. Additionally, in the Appendix, we present detailed tables for individual oligomers containing the excitation energies and many-particle wave functions of important excited states, as well as corresponding transition dipoles.

1. Naphthalene

In Fig. 3 we present the linear optical absorption spectra of naphthalene computed with the FCI method, using both the standard and screened parameters in the PPP Hamiltonian. The wave functions of the excited states contributing to various peaks are presented in Tables III and IV in the Appendix. Since these calculations were performed using the FCI approach, they are exact within the model chosen and cannot be improved. Therefore, any discrepancy which these results may exhibit with respect to the experiments is a reflection of the limitations of the model or the parameters used, and not that of the correlation approach.

From Fig. 3 and Tables III and IV, it is obvious that the first peaks of the spectra calculated with the standard and screened parameters are in excellent qualitative and quanti-

TABLE II. Comparison of results of our calculations performed with the standard (Std.) parameters and the screened (Scd.) parameters with other experimental and theoretical results for the three most important low-lying states. For Ref. 51 (Kadantsev *et al.*), results quoted with the asterisk (*) correspond to their CISD calculations, while those without it are their B3LYP results.

	Excitation energy (eV)			
	Present work			
State	Std. para.	Scd. para.	Experimental	Other theoretical
			Naphthalene ($C_{10}H_8$)	
$1B_{3u}^-$	3.61	3.22	3.97,[a] 4.03,[b] 4.0[c]	4.02,[d] 3.74,[e] 3.60,[f] 4.44,[g] 4.49,[g*] 4.21,[h] 4.46,[i] 4.09[j]
$1B_{2u}^+$	4.45	4.51	4.34,[a] 4.38,[b] 4.45,[c] 4.46[k]	4.49,[d] 4.54,[e] 4.46,[f] 4.35,[g] 5.27,[g*] 4.12,[h] 4.88,[i] 4.62[j]
$1B_{3u}^+$	5.99	5.30	5.64,[a] 5.62,[b] 5.89,[c] 5.95[k]	5.94,[d] 5.84,[e] 5.85,[g] 6.24,[g*] 5.69,[h] 5.62[j]
			Anthracene ($C_{14}H_{10}$)	
$1B_{3u}^-$	3.25	2.91	3.47,[a] 3.57,[b] 3.72[l]	3.72,[d] 3.22,[e] 3.23,[m,n] 3.84,[g] 3.93,[g*] 3.60,[h] 3.89[i]
$1B_{2u}^+$	3.66	3.55	3.31,[a] 3.38,[b] 3.42,[l,o] 3.43[p]	3.65,[d,q] 3.60,[e] 3.68,[n] 3.40,[m] 3.21,[g] 4.05,[g*] 2.96,[h] 3.69[i]
$1B_{3u}^+$	5.34	4.64	4.83,[a] 4.86,[b] 5.24[o,r]	5.50,[d] 5.27,[e] 5.36,[n] 4.77,[m] 5.35,[q] 5.14,[g] 5.49,[g*] 4.93[h]
			Tetracene ($C_{18}H_{12}$)	
$1B_{3u}^-$	3.22	3.02	3.16,[a] 3.32,[b] 3.12[s]	3.57,[d] 3.04,[e] 2.92,[m] 3.46,[g] 3.58,[g*] 3.21,[h] 3.52[i]
$1B_{2u}^+$	3.16	2.97	2.60,[a,t] 2.71,[b] 2.72,[s] 2.63[u]	3.11,[d] 3.05,[e] 2.80,[m] 2.44,[g] 3.22,[g*] 2.19,[h] 2.90[i]
$1B_{3u}^+$	5.01	4.38	4.55,[a] 4.52,[b] 4.50,[t] 4.51[u]	5.09,[d] 4.86,[e] 4.32,[m] 4.63,[g] 4.96,[g*] 4.38[h]
			Pentacene ($C_{22}H_{14}$)	
$1B_{3u}^-$	3.17	2.99	2.96,[a] 3.05,[b] 2.89,[u] 3.73[v]	3.51,[d] 2.99,[e] 3.20,[g] 3.34,[g*] 2.95,[h] 3.12[i]
$1B_{2u}^+$	2.86	2.65	2.14,[a] 2.23,[b] 2.12,[u] 2.28[v]	2.81,[d] 2.70,[e] 1.90,[g] 2.64,[g*] 1.65,[h] 2.37[i]
$1B_{3u}^+$	4.73	4.22	4.01,[a] 4.10,[u] 4.40[v]	4.80,[d] 4.57,[e] 4.24,[g] 4.57,[g*] 3.96[h]
			Hexacene ($C_{26}H_{16}$)	
$1B_{3u}^-$	3.07	2.77	2.80,[b] 2.67[w]	3.34,[w] 3.01,[g] 3.17,[g*] 2.76,[h] 2.87[i]
$1B_{2u}^+$	2.71	2.38	1.90,[b] 1.91[w]	2.18,[w] 1.50,[g] 2.23,[g*] 1.25,[h] 2.02[i]
$1B_{3u}^+$	4.61	4.07	3.94[w]	4.05,[w] 3.94,[g] 4.27,[g*] 3.64[h]
			Heptacene ($C_{30}H_{18}$)	
$1B_{3u}^-$	2.73	2.35		2.35[h]
$1B_{2u}^+$	2.63	2.24		0.94[h]
$1B_{3u}^+$	4.48	3.80		3.36[h]

[a]Reference 11.
[b]Reference 12.
[c]Reference 16.
[d]Reference 44.
[e]Reference 46.
[f]Reference 73.
[g]Reference 51.
[h]Reference 54.
[i]Reference 52.
[j]Reference 79.
[k]Reference 17.
[l]Reference 23.
[m]Reference 48.
[n]Reference 74.
[o]Reference 25.
[p]Reference 22.
[q]Reference 7.
[r]Reference 24.
[s]Reference 30.
[t]Reference 31.
[u]Reference 32.
[v]Reference 36.
[w]Reference 42.

tative agreement with each other. The second peak computed using the standard parameters is due to both the *x*-polarized and *y*-polarized components, but it is obvious from the Table III that the *x*-polarized component dominates. However, with the screened parameters, it gets dissociated into two separate features II and III with *x*-polarized and *y*-polarized components, respectively. Qualitatively, both spectra are in good agreement with each other (see Tables III and IV). Regarding the quantitative aspects, one notices that the excitation energies computed with the screened parameters are redshifted as compared to those computed with the standard parameters. This is in agreement with results obtained for other conjugated polymers as well.[60,62–64]

Comparison of our results for naphthalene, for the invisible (dipole-forbidden) $1B_{3u}^-$ state and the first two visible $1B_{2u}^+$ and $1B_{3u}^+$ states with the experimental ones and those of other calculations is presented in Table II. Although several other experimental results on optical absorption in naphthalene exist,[11–13,15–19] here we compare our results with the experimental results of Huebner *et al.*[16] and Aleksandrovsky *et al.*,[17] who performed experiments on the gas phase of naphthalene. Since we have performed calculations on isolated oligomers, therefore, the most appropriate comparison of our results will be with the data obtained by gas-phase experiments. Huebner *et al.*[16] suggested $1B_{2u}^+$ and $1B_{3u}^+$ states at 4.45 eV and 5.89 eV, respectively, while Aleksandrovsky

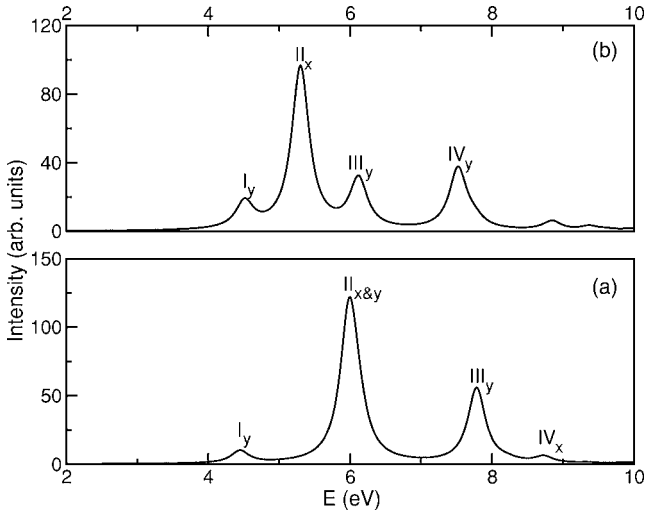

FIG. 3. Linear optical absorption spectrum of naphthalene computed with (a) standard parameters and (b) screened parameters in the PPP model Hamiltonian. The FCI method was used for the purpose. A linewidth of 0.15 eV was assumed. As a subscript of each feature, its polarization is also mentioned. Thus, e.g., III_y implies that peak III is short-axis polarized.

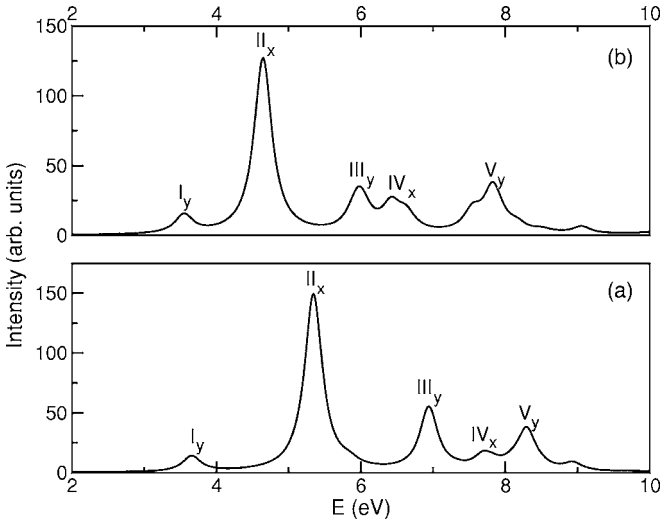

FIG. 4. Linear optical absorption spectrum of anthracene computed with (a) standard parameters and (b) screened parameters. The FCI method coupled with the PPP model Hamiltonian was used for the purpose. A linewidth of 0.15 eV was assumed. As a subscript of each feature, its polarization is also mentioned.

et al.[17] mentioned these states to be at 4.46 eV and 5.95 eV, respectively. Thus, our results on the relative ordering of the $1B_{2u}^+$ and $1B_{3u}^+$ states in the spectra, using standard parameters, are in excellent agreement with the results of Huebner *et al.*[16] and the recent experiment of Aleksandrovsky *et al.*[17] The screened parameters slightly overestimate the experimental results[16,17] for the $1B_{2u}^+$ state and underestimate them for the $1B_{3u}^+$ state. Excellent agreement between our results and those of the recent experimental results of Aleksandrovsky *et al.*[17] testifies to the essential correctness of the PPP model to the naphthalene with standard parameters. The dipole-forbidden $1B_{3u}^-$ state has not been discussed by Aleksandrovsky *et al.* but Huebner *et al.* suggested this feature to be at 4.0 eV, which is higher as compared to both of our results. Thus, both sets of calculations appear to capture the qualitative features of the spectra quite well; however, quantitatively, standard parameter calculations appear to be more accurate upon comparison with the experiments.[16,17]

Several theoreticians have studied the low-lying excited states of naphthalene.[8,44,46,47,51,52,54,56,57,73,76–79] The results obtained from our standard set of parameters for the $1B_{2u}^+$ and $1B_{3u}^+$ states are in perfect agreement with the calculations performed by Pariser[44] and Ramasesha and Soos.[73] Also, they agree quite well with the recent calculations performed by Kadantsev and co-workers,[51] using B3LYP as exchange-correlation (xc) functional. The dipole forbidden $1B_{3u}^-$ state is obtained at lower energy than calculated by Pariser[44] and Kadantsev and co-workers,[51] but is in excellent agreement with the results of Ramasesha and Soos.[73]

2. Anthracene

An anthracene molecule contains 14 π electrons, which is quite a large system for the application of the FCI approach. However, FCI calculations using the PPP model have been performed by Ramasesha *et al.*[74] for anthracene, but they did not report its linear absorption spectrum. Therefore, in our present work we have computed the linear absorption spectrum of the anthracene using the FCI approach and have also discussed the nature of low-lying excited states contributing to the spectrum.

Figure 4 presents the linear optical absorption spectra of anthracene computed using the FCI method, along with the standard and screened sets of parameters in the PPP Hamiltonian. The wave functions of the excited states contributing to various peaks are presented in Tables V and VI in the Appendix.

In our calculations on anthracene using standard parameters, the first peak of the spectrum was identified as the $1B_{2u}^+$ state at 3.66 eV, while the most intense feature of the spectrum corresponding to the $1B_{3u}^+$ state was obtained at 5.34 eV. The dipole-forbidden $1B_{3u}^-$ state was obtained at 3.25 eV, and its wave function contains both singly and doubly excited configurations. Using screened parameters, we obtained $1B_{3u}^-$, $1B_{2u}^+$, and $1B_{3u}^+$ states at 2.91 eV, 3.55 eV, and 4.64 eV, respectively. Thus, calculations performed with both sets of PPP parameters predict the dipole-forbidden $1B_{3u}^-$ state at lower energies than the $1B_{2u}^+$ state.

Comparison of our theoretical results to the experimental and theoretical results of other authors is presented in Table II. Several experimental investigations of the absorption spectra of anthracene have been performed over the years. For the $1B_{2u}^+$ state, our results with both sets of parameters overestimate the experimental results of Klevens and Platt (3.31 eV),[11] Biermann and Schmidt (3.38 eV),[12] Lambert *et al.* (3.43 eV),[22] Dick and Hohlneicher (3.42 eV),[23] and Man *et al.* (3.424 eV).[25] Comparatively speaking, however, the result obtained from screened parameters is in slightly better agreement with the experimental results.

Lambert *et al.*[22] studied the isolated molecules of anthracene using jet spectroscopy, while Dick and Hohlneicher[23]

observed the low-lying excited states of anthracene in the gas phase. Thus, our calculations, which were performed on isolated oligomers, are directly comparable to these two experimental results. The most intense feature of the spectra, which corresponds to the $1B_{3u}^{+}$ state was obtained at 5.34 eV from standard parameters while screened parameters suggested this state to be at 4.64 eV. Our result with standard parameters agrees well with the results obtained by Man *et al.*[25] and Lyons and Morris[24] They both suggested this state to be at 5.24 eV. Our screened parameter result is in good agreement with the result of Klevens and Platt[11] and Biermann and Schmidt[12] for the $1B_{3u}^{+}$ state, who suggested this state to be at 4.83 eV and 4.86 eV, respectively.

Our correlated value of 3.25 eV for the excitation energy of the $1B_{3u}^{-}$ state obtained using the standard parameters is in fairly good agreement with the experimental results of Klevens and Platt (3.47 eV) (Ref. 11) and Biermann and Schmidt (3.57 eV).[12] However, it is lower as compared to the experimental results of Dick and Hohlneicher (3.72 eV).[23] Our screened parameter results (2.91 eV) obviously significantly underestimate the experimental excitation energy of the $1B_{3u}^{-}$ state. Thus, we observe that for some states our standard parameter results agree well with the experiments, while for other states the screened parameter results are in better agreement with the experiments. However, the standard-parameter-based results are in better overall agreement with the gas-phase experiments, as compared to those obtained using screened parameters.

Next we discuss and compare our results with the results of calculations performed by other theoreticians. Our correlated results obtained by using standard parameters for $1B_{3u}^{-}$, $1B_{2u}^{+}$, and $1B_{3u}^{+}$ states are in perfect agreement with the results obtained by Ramasesha[74] using the FCI methodology with PPP model Hamiltonian. Again, this perfect agreement proves the essential correctness of our calculations. The $1B_{2u}^{+}$ state obtained using standard parameters shows excellent agreement with the pioneering work of Pariser,[44] who performed SCI calculations. However, energetically both $1B_{3u}^{+}$ (dipole-allowed) and $1B_{3u}^{-}$ (dipole-forbidden) states obtained from our calculations are lower than those reported by Pariser.[44] This clearly is due to the superior treatment of electron correlations in our work. Additionally, the results for the $1B_{2u}^{+}$ and $1B_{3u}^{+}$ states are in excellent agreement with the results of Hummer *et al.*[7] and in close agreement with the recent results of Kadantsev and co-workers,[51] obtained using B3LYP as xc functional. Recently, Kawashima and co-workers[48] performed calculations on linear absorption in anthracene using the *ab initio* MRMP methodology. The energies they obtained for the $1B_{2u}^{+}$ state (3.40 eV) and $1B_{3u}^{+}$ state (4.77 eV) are quite close to our screened parameter results and slightly less than the results obtained from our calculations using standard parameters. They mentioned the $1B_{3u}^{-}$ state at 3.23 eV, which is in perfect agreement with the results that we have obtained using standard parameters, while it is higher than the value that we have obtained using screened parameters (2.91 eV). A few other theoretical results of other authors are also given in Table II for the sake of comparison.

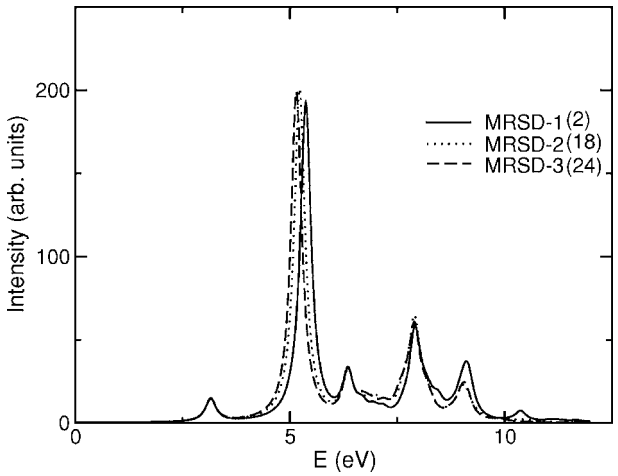

FIG. 5. Convergence of the linear absorption spectrum of tetracene, computed using the MRSDCI method (standard parameters) with respect to number of reference configurations (N_{ref}). The numbers written in the parentheses represent N_{ref} included in the corresponding MRSDCI calculations.

3. Tetracene

The next member of the polyacene family is tetracene, which contains 18 π electrons. Because of the relatively larger number of π electrons in the system, it is virtually impossible to use the FCI method for the present system. Thus, we used the QCI technique for computing the ground state and the low-lying excited states corresponding to the short-axis polarized transitions (B_{2u}-type states), while the MRSDCI methodology was used for the excited states which correspond to the long-axis polarized transitions (B_{3u}-type states). The reason behind using different CI techniques is that the QCI method can only be used for single reference states such as the ground state ($1A_g$) and the B_{2u}-type states, while from Tables III–VI in the Appendix, it is obvious that B_{3u} states are multireference states with two dominant configurations for which the QCI method cannot be used. Therefore, for states of B_{3u} symmetry, the MRSDCI method has been used.

In order to demonstrate the convergence of our MRSDCI calculations, we present the spectra in Fig. 5, calculated with increasing number of reference configurations (N_{ref}). It is obvious from the figure that the spectrum computed using 24 reference configurations is in very good agreement with the spectrum computed using 18 reference configurations, implying that convergence with respect to N_{ref} has been achieved. We would also like to mention that the accuracy of the MRSDCI method was demonstrated in our earlier works where the results obtained using that approach were found to be in excellent agreement with the experiments.[59–61]

Tetracene has been studied by several theoreticians[8,44,46,48,50–52,54–57,76,80] as well as experimentalists.[11,12,29–34] The linear absorption spectra of tetracene, computed using standard and screened parameters, are presented in Fig. 6. The excited states together with the corresponding energies, transition dipoles, and wave functions are presented in Tables VII and VIII.

The first peak of the correlated spectra was obtained at 3.16 eV and 2.97 eV, using the standard parameters and the

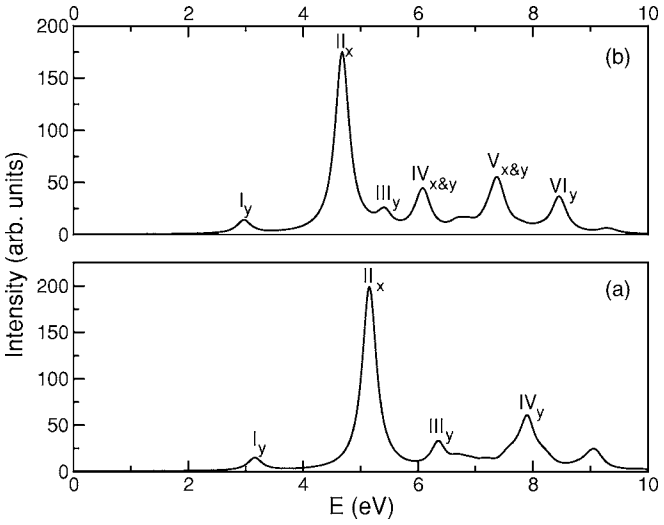

FIG. 6. Linear optical absorption spectrum of tetracene computed with (a) standard parameters and (b) screened parameters. The QCI method was used to compute the ground state ($1A_g^-$ state) and B_{2u}^+ states, while the MRSDCI method was used to compute the B_{3u}^+ states.

screened parameters, respectively, and corresponds to the $1B_{2u}^+$ state of the oligomer. The second peak, which is also the most intense feature in both the spectra, corresponds to the $1B_{3u}^+$ state. The dipole-forbidden $1B_{3u}^-$ state has been obtained at higher energy than the $1B_{2u}^+$ state (cf. Tables VII and VIII) in the Appendix, which is different as compared to naphthalene and anthracene, but in agreement with the results of other investigators (cf. Table II).

The comparison of our calculated results for $1B_{3u}^-$, $1B_{2u}^+$, and $1B_{3u}^+$ excited states with the several experimental and other calculated results is present in Table II. Our standard parameter results generally overestimate the excitation energies when compared to the experiments, while the agreement between the screened parameters results and the experiments[11,12,30–32] is much better.

The $1B_{2u}^+$ excitation energies computed using the standard as well as the screened parameters overestimate all the experimental results.[11,12,29–32] Yet our screened parameter value of the excitation energy of the $1B_{2u}^+$ state (2.97 eV) is in reasonably good agreement with the experimental values of Klevens and Platt (2.60 eV),[11] Biermann and Schmidt (2.71 eV),[12] Bree and Lyons (2.60 eV),[31] Birks (2.63 eV),[32] and Berlman (2.72 eV).[30] As far as the $1B_{3u}^+$ state is concerned, our screened parameter value of 4.38 eV is fairly close to the several experimental values reported to be near 4.50 eV.[11,12,31,32] However, our standard parameter value of 5.01 eV for the same overestimates the experiments by about 0.5 eV. Our results for the dipole-forbidden $1B_{3u}^-$ state with both sets of parameters are in good agreement with the experiments. As compared to the experiments of Klevens and Platt[11] and Berlman,[30] our standard parameter excitation energy for the $1B_{3u}^-$ state is slightly higher, while the screened parameter value is slightly lower. Thus, we can conclude that in the case of tetracene, for all the three excited states discussed, screened-parameter-based calculations provide better agreement with the experiments.

On comparing our results with other theoretical results we find that the $1B_{2u}^+$ and $1B_{3u}^+$ states, computed using standard parameters, are in excellent agreement with the benchmark work of Pariser,[44] while the $1B_{3u}^-$ state has been computed at a lower value by both of our parameters. Ramasesha and co-workers also computed the optical gap of tetracene using the PPP model Hamiltonian coupled with the DMRG technique.[50] They reported the $1B_{2u}^+$ state at 3.20 eV, which is in perfect agreement with the $1B_{2u}^+$ state computed by us using the standard parameters. The results obtained using screened parameters for all the compared states are in very good agreement with the results of Ham and Ruedenberg[46] and with the *ab initio* MRMP-based results of Kawashima *et al.*[48] The results of Kadantsev and co-workers[51] obtained using B3LYP as xc functional for the *x*-polarized states $1B_{3u}^-$ and $1B_{3u}^+$ are higher than our results of the screened parameters, while they are at low energy for the *y*-polarized $1B_{2u}^+$ state.

4. Pentacene

The most thoroughly studied and most widely used member of the polyacene family is pentacene. It has been quite famous in recent years due to its use in thin-film growth of electronic devices.[81–83] It is among the most promising organic molecular semiconductors due to its high charge carrier mobility.[1–3] It has been studied by several researchers to understand the nature of its low-lying excited states. However, most of the experimentalists have mainly reported the energy corresponding to the $1B_{2u}^+$ state.[29,34,35,37–41] As per our knowledge, experimentally only Klevens and Platt,[11] Biermann and Schmidt,[12] and Birks[32] have performed extensive studies of the $1B_{3u}^-$, $1B_{2u}^+$, and $1B_{3u}^+$ excited states. Additionally, Halasinski *et al.*[36] measured the vibronic transitions of neutral pentacene isolated in Ne, Ar, and Kr matrices and reported the data corresponding to the $1B_{3u}^-$, $1B_{2u}^+$, and $1B_{3u}^+$ excited states.

Theoretically, the low-lying states of pentacene have been studied by several scientists using various methodologies.[8,44,46,50,56,57,84] Similar to tetracene, for pentacene also we used the QCI method for computing the ground state ($1A_g$) and the B_{2u}-type excited states, while the B_{3u}-type excited states were computed using the MRSDCI technique.

In Fig. 7 we present the linear optical absorption spectra computed using both standard and screened parameters in the PPP model Hamiltonian. The energies and wave functions corresponding to the visible features in the spectra as well as $1B_{3u}^-$ state are presented in Tables IX and X in the Appendix.

The first peak, as usual, corresponds mainly to the $1B_{2u}^+$ state, while the second peak is a mixture of states corresponding to *x*-polarized and *y*-polarized photons. But as is clear from the transition dipoles, the intensity of the peak is mainly due to *x*-polarized photons corresponding to $H \rightarrow L+2+$c.c. excitations leading to the $1B_{3u}^+$ state (see Tables IX and X).

The comparison of our results with other theoretical and experimental results is presented in Table II. On comparing our results with the experimental results we found that on most occasions both sets of parameters overestimate the ex-

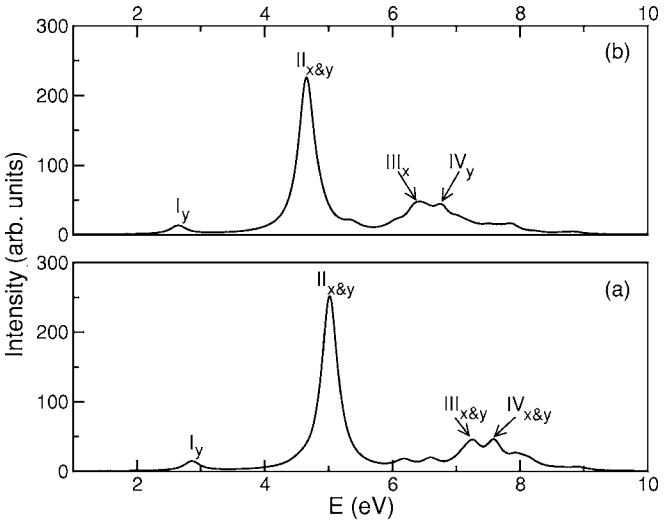

FIG. 7. Linear optical absorption spectrum of pentacene computed with (a) standard parameters and (b) screened parameters. The QCI method was used to compute the B_{2u}^+ states, while the MRSDCI method was used to compute the B_{3u}^+ states.

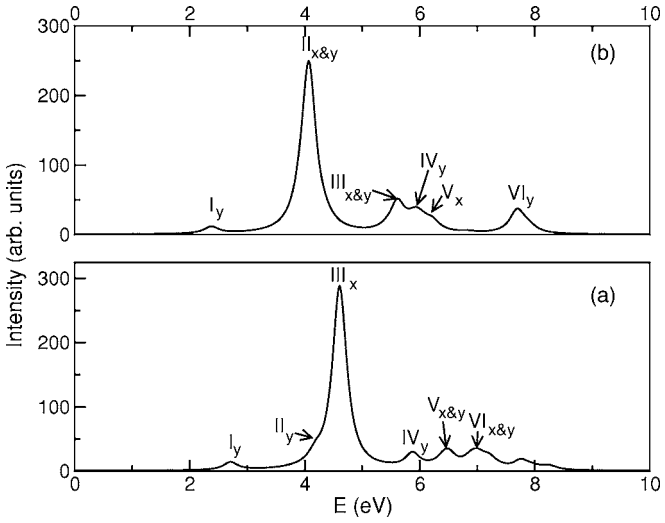

FIG. 8. Linear optical absorption spectrum of hexacene computed with (a) standard parameters and (b) screened parameters. The MRSDCI method was used to include the electron-correlation effects.

perimental results. However, overall, the results obtained using the screened parameters are in much better agreement with the experiments. For example, the screened parameter results on $1B_{2u}^+$ and $1B_{3u}^+$ states are in very good agreement with the experiments of Klevens and Platt,[11] Biermann and Schmidt,[12] Birks,[32] and Halasinski *et al.*[36] However, several experimentalists have reported that the $1B_{2u}^+$ state lies between 1.7 eV and 1.9 eV.[37–41] The difference in our calculated results and these experimental results could be due to bulk effects, as most of these experiments were performed on bulk pentacene, thus possibly explaining the substantially lower values of band gaps. We again emphasize that our calculations were performed on a single molecule of pentacene, leading to comparatively larger excitation energies.

Next, we compare our results with the theoretical results of other authors. Our correlated results for $1B_{2u}^+$ and $1B_{3u}^+$ obtained using standard parameters are in very good agreement with Pariser[44] while the energy corresponding to the $1B_{3u}^-$ state is obtained to be lower in our standard parameter calculations. Our standard parameter value of the $1B_{2u}^+$ excitation energy (2.86 eV) is also in excellent agreement with the value 2.92 eV obtained by Raghu *et al.*[50] from their DMRG calculations. Our results obtained using screened parameters are in very good agreement with the results obtained by Ham and Ruedenberg[46] They used free-electron molecular orbital (FE MO) theory to compute the energies of the low-lying excited states. From our screened parameter calculations, the energy obtained for the $1B_{3u}^-$ excited state is in perfect agreement with the results of Ham and Ruedenberg,[46] while the energies of $1B_{2u}^+$ and $1B_{3u}^+$ excited states are slightly less than that of Ham and Ruedenberg[46] The energies of the *x*-polarized $1B_{3u}^-$ and $1B_{3u}^+$ states obtained using standard as well as screened parameters agree well with the results for these states calculated by Kadantsev and co-workers[51] using the xc functional. Recently, Tiago *et al.*[84] computed the energy gap for solution-phase-crystallized (S) structure and vapor-phase-crystallized (V) structure of pentacene using the *ab initio* pseudopotential density functional method and GW approach. They obtained the energy gap to be 2.2 eV for S structure while 1.9 eV for V structure. This low value of energy can be understood due to the bulk effects. Thus, their calculation supports our belief that bulk effects affect the $H \rightarrow L$ gap significantly.

5. Hexacene

With the increase in the size of oligoacene, it becomes less stable, poorly soluble, and more reactive.[85–90] Thus, preparation and practical study of higher acenes like hexacene is a difficult task.[67,91] To the best of our knowledge, experimentally hexacene has only been studied by Biermann and Schmidt[12] and Angliker *et al.*[42] They measured the absorption spectra of hexacene in solution. Angliker *et al.*[42] have also computed the low-lying excited states by performing PPP SCF-SCI calculations. Most recently, Grimme and Parac,[52] Heinze *et al.*,[54] and Houk *et al.*[55] have also calculated the low-lying excited states using time-dependent density-functional-theory- (TDDFT-) based approaches.

In Fig. 8, we present the linear absorption spectra of hexacene, computed using both standard and screened parameters in the PPP model Hamiltonian. For inclusion of electron-correlation effects, the MRSDCI method was employed for all the states involved. The excited states, corresponding energies, transition dipoles, and wave functions of the various features of the spectra are presented in Tables XI and XII in the Appendix. The spectrum obtained using standard parameters predicts the $1B_{2u}^+$ state at 2.71 eV, while from screened parameters it was obtained at 2.38 eV. In both cases, the intensity of this peak (peak I) is quite small. In the standard parameter spectrum [cf. Fig. 8(a)], the second peak corresponding to the $1B_{3u}^+$ state is preceded by a weak shoulder (II_y) which is due to a *y*-polarized photon and has been identified as the $2B_{2u}^+$ state.

In the screened parameter spectrum, this state is almost degenerate with the $1B_{3u}^+$ state and is part of the main feature

II in the spectrum. However, with both sets of parameters, the intensity is mainly due to the *x*-polarized photon (see Tables XI and XII).

The remarkable feature of the dipole-forbidden $1B_{3u}^-$ state for hexacene is that its wave function mainly consists of double excitations, with the single excitations making smaller contributions. This is quite unlike the smaller acenes in which the $1B_{3u}^-$ state consists mainly of singly excited configurations. Thus, for this state, the contribution of correlation effects appears to increase with size of the oligoacene.

Angliker *et al.*[42] have studied the spectra of hexacene experimentally as well as theoretically. They dissolved the hexacene in silicone oil and measured the $1B_{2u}^+$, $1B_{3u}^-$, and $1B_{3u}^+$ excited states at 1.91 eV, 2.67 eV, and 3.94 eV, respectively. Theoretically they computed these states using the PPP SCF-SCI method at 2.18 eV, 3.34 eV, and 4.05 eV, respectively. Our correlated calculations using standard parameters computed these states at 2.71 eV, 3.07 eV, and 4.61 eV, respectively, while screened parameters found these states to be at 2.38 eV, 2.77 eV, and 4.07 eV, respectively. Thus, generally our standard parameter calculations overestimate the experimental results of Angliker *et al.*[42] for the $1B_{3u}^-$ state. However, with the screened parameters, our results are in good agreement with their experimental results[42] for the $1B_{3u}^-$ and $1B_{3u}^+$ excited states. Our screened parameter results for the $1B_{2u}^+$ and $1B_{3u}^+$ states also agree well with their calculated results.[42] Biermann and Schmidt[12] observed $1B_{3u}^-$ at 2.80 eV and $1B_{2u}^+$ at 1.90 eV—thus, in very good agreement with our screened parameter results for the first DF *x*-polarized state, while slightly overestimated for the first *y*-polarized state. Again, the trend is clear that the results obtained using the screened parameters are in better agreement with the experiments.[42]

Recently, Grimme and Parac[52] used TDDFT and reported $1B_{3u}^-$ and $1B_{2u}^+$ states at 2.87 eV and 2.02 eV, which is in close agreement with our screened parameter results. Heinze *et al.*[54] calculated the low-lying excited states of polyacenes using TDDFT-based coupled Kohn-Sham (CKS) methodology. They report the $1B_{2u}^+$, $1B_{3u}^+$, and $1B_{3u}^-$ states to be at 1.25 eV, 3.64 eV, and 2.76 eV, respectively. Kadantsev and co-workers[51] reported these states to be at 1.50, 3.94, and 3.01 eV, respectively. Except for the $1B_{2u}^+$ state, our results of screened parameter calculations are in very good agreement with their results. Additionally, Houk *et al.*[55] computed the HOMO to LUMO gap ($1B_{2u}^+$ state in our notation) at 1.54 eV, using the TDDFT approach. The lower value of the $1B_{2u}^+$ excitation energy from the TDDFT calculations could be due to the usual problem of underestimating the band gaps, associated with DFT-based approaches.

6. Heptacene

The final member of the oligoacene family which we have studied is heptacene. It is a large molecule with seven diffused benzene rings and 30 π electrons. It is an inherently unstable molecule,[92] whose synthesis has been controversial.[93] Initially, Clar[94] and Marschalk[95] claimed the preparation of heptacene successfully. Later, Bailey and Liaio reported the only other successful synthesis of heptacene.[96] Just two years after the report of Bailey and Liaio, Clar retracted his earlier claim,[94] and now it is commonly agreed that heptacene cannot be prepared in a pure state.[97,98] Therefore, no experimental data are available to date for the low-lying excited states of heptacene. However, the low-lying excited states have been studied theoretically by a few researchers using the TDDFT method.[54,55]

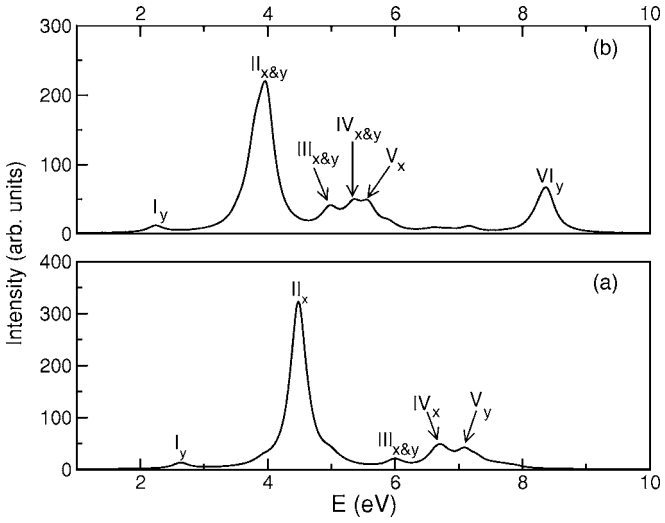

FIG. 9. Linear optical absorption spectrum of heptacene computed with (a) standard parameters and (b) screened parameters. The MRSDCI method, coupled with the PPP model Hamiltonian, was used for the purpose.

We computed the linear absorption spectra of heptacene using standard and screened parameters in the PPP model Hamiltonian, together with the use of the MRSDCI technique for the inclusion of correlation effects. The calculated spectra are presented in Fig. 9, while Tables XIII and XIV in the Appendix provide detailed information regarding the excited-state properties. We note that, similar to the case of hexacene, the excited-state wave functions of the $1B_{3u}^+$ and $1B_{3u}^-$ states are fundamentally different in that the $1B_{3u}^+$ state consists mainly of one-particle excitations, while the $1B_{3u}^-$ state is dominated by a double excitation, irrespective of the choice of Coulomb parameters.

The first feature of Fig. 9, corresponding to the $1B_{2u}^+$ state, was obtained at 2.63 eV from standard parameter calculations and at 2.24 eV on using the screened parameters in the PPP Hamiltonian. The dipole-forbidden $1B_{3u}^-$ state was obtained at 2.73 eV from the standard parameters and at 2.35 eV from the screened parameters. By both parameters $1B_{3u}^-$ is at higher energy than $1B_{2u}^+$, as is the case from tetracene onwards. Heinze *et al.*[54] also calculated the excitation energies for heptacene using the TDDFT-based CKS methodology.[54] They predicted the $1B_{2u}^+$ state at 0.943 eV, $1B_{3u}^-$ state at 2.349 eV, and $1B_{3u}^+$ state at 3.363 eV. Additionally, Houk *et al.*[55] used the TDDFT method and computed the $1B_{2u}^+$ state (HOMO to LUMO gap) at 1.24 eV. Our $1B_{2u}^+$ state is higher in comparison to both DFT-based results. Lower values of energy for the $1B_{2u}^+$ state obtained by the DFT-based methodology could be due to their well-known problem of underestimating the band gaps. The dipole-forbidden $1B_{3u}^-$ states computed by us, using screened parameters, are in perfect agreement with the results of Heinze *et*

al.,[54] while the visible $1B_{3u}^{+}$ state with maximum intensity is obtained at higher energies by both standard and screened parameters.

IV. CONCLUSIONS

In this paper we presented a large-scale correlated study of linear optical absorption and low-lying excited states of oligoacenes ranging from naphthalene to heptacene using the PPP model Hamiltonian. In order to investigate the influence of the Coulomb parameters on the computed properties, these calculations were performed with two sets of parameters in the PPP model: (i) standard Ohno parameters[65] and (ii) a screened set of parameters.[66] An extensive comparison of our correlated results was made with (i) the results obtained using the single-particle Hückel model, (ii) the experimental results, and (iii) the theoretical results of other authors. Next, in a unified manner, we present the conclusions which can be drawn from our calculations.

Qualitatively speaking, some aspects of the linear optical spectrum computed using the Hückel model were found to be very similar to the one computed using the PPP model for all the oligoacenes investigated. For example, with both sets of calculations, the first peak of the spectrum corresponded to the $1B_{2u}^{+}$ state, while the second, and the most intense, peak of the spectrum corresponded to the $1B_{3u}^{+}$ state for all acenes. Both sets of calculations also predicted diminishing relative intensity of the $1B_{2u}^{+}$ with increasing conjugation length. Additionally, irrespective of the parameters used in the PPP model or the size of the acene involved, the many-particle wave function of the $1B_{2u}^{+}$ state in all cases consisted mainly of the $H \rightarrow L$ excitation, in excellent agreement with the Hückel model results. However, quantitatively speaking, for all the oligoacenes, the optical gaps computed using the Hückel model were much smaller than their PPP, and experimental, counterparts.

As far as the relative position of the dipole-forbidden $1B_{3u}^{-}$ excited state is concerned, with both sets of Coulomb parameters the following trends were observed: (i) for oligoacenes up to anthracene, the $1B_{3u}^{-}$ state occurs below the $1B_{2u}^{+}$ state; however, (ii) from tetracene onwards the relative ordering of the two states gets reversed and the $1B_{2u}^{+}$ state begins to occur below $1B_{3u}^{-}$. This theoretical result was found to be in good agreement with most of the experiments. Additionally, the influence of the electron correlation effects on the $1B_{3u}^{-}$ state appears to get stronger with increasing size of the acene involved. This manifests itself in the form of the trend that the contribution of the singly excited configurations to the many-particle wave function of $1B_{3u}^{-}$ decreases with the increasing conjugation length and is eventually overshadowed by the doubly excited configurations for the larger acenes.

As mentioned earlier, for all oligomers studied, irrespective of the Coulomb parameters used in the PPP Hamiltonian, the $1B_{3u}^{+}$ state was found to be the most intense peak of the spectrum, in excellent agreement with all available experiments. Additionally, unlike the $1B_{3u}^{-}$ state, for all acenes, the many-particle wave function of this most intense peak was dominated mainly by singly excited configurations, although with increasing conjugation length the relative contribution of the doubly excited configurations to the $1B_{3u}^{+}$ appears to increase. Therefore, it is conceivable that for conjugation lengths longer than the ones considered here, the contributions of the double excitations to $1B_{3u}^{+}$ could overshadow those of the single excitations. Yet, for a given conjugation length, the electron-correlation effects as judged from the relative contribution of the double excitations, appear to be stronger in the case of the $1B_{3u}^{-}$ state, as compared to the $1B_{3u}^{+}$ state.

Finally, we discuss the issue pertaining to the choice of Coulomb parameters for the PPP model when it comes to describing the linear optical properties of oligoacenes. We notice that in an overall sense, with increasing conjugation length, the results obtained using the screened parameters are in better quantitative agreement with the experiments as compared to those obtained using the standard parameters. There were some acenes for which both parameters gave reasonable results, with the screened parameter energies slightly lower than the experimental energies and the standard parameter ones slightly higher. Recalling that screened parameters are generally used to describe solid-state or solvent effects (interchain screening), the better quantitative agreement obtained using the screened parameters for the longer acenes, in our opinion, suggests the increasing importance of solid-state effects on longer acenes.

In this paper we restricted ourselves to the low-lying excited states of polyacenes which contribute to their linear optical properties. However, it will also be interesting to explore the nature of their two-photon states, which will contribute to the nonlinear, as well as excited-state, absorption in these materials. Given the inherent anisotropy (short axis versus long axis) of these materials, several types of intermediate states will possibly govern their nonlinear optical response. At present, studies along these directions are underway by our group.

ACKNOWLEDGMENTS

We thank the Department of Science and Technology (DST), Government of India, for providing financial support for this work under Grant No. SP/S2/M-10/2000.

APPENDIX: EXCITED-STATE PROPERTIES

Here we present the tables summarizing the results of our CI calculations for various oligoacenes. The data presented in the tables include important configurations contributing to the many-body wave functions of various excited states, their excitation energies, and transition dipoles connecting them to the ground state. The results are presented in separate subsections corresponding to each oligoacene and include calculations performed with both standard parameters and the screened set of parameters in the PPP model.

Naphthalene

TABLE III. Excited states contributing to the linear absorption spectrum of naphthalene computed using the FCI method coupled with the standard parameters in the PPP model Hamiltonian. The table includes many-particle wave functions, excitation energies, and dipole matrix elements of various states with respect to the ground state. DF corresponds to the dipole-forbidden state. "+c.c." indicates that the coefficient of the charge conjugate of a given configuration has the same sign, while "−c.c." implies that the two coefficients have opposite signs.

Peak	State	E (eV)	Transition dipole (Å)	Wave functions
DF	$1B_{3u}^{-}$	3.61	0.000	$\|H\rightarrow L+1\rangle$+c.c.(0.6235)
				$\|H\rightarrow L+1;H-3\rightarrow L\rangle$+c.c.(0.1345)
				$\|H-2\rightarrow L+3\rangle$+c.c.(0.1107)
I	$1B_{2u}^{+}$	4.45	0.551	$\|H\rightarrow L\rangle$(0.8773)
				$\|H-1\rightarrow L+1\rangle$(0.3521)
II	$1B_{3u}^{+}$	5.99	1.638	$\|H\rightarrow L+1\rangle$−c.c.(0.6524)
				$\|H\rightarrow L+1;H-3\rightarrow L\rangle$−c.c.(0.1015)
	$2B_{2u}^{+}$	6.10	0.739	$\|H-1\rightarrow L+1\rangle$(0.8011)
				$\|H\rightarrow L\rangle$(0.2958)
				$\|H-2\rightarrow L+2\rangle$(0.2952)
III	$3B_{2u}^{+}$	7.78	1.028	$\|H-2\rightarrow L+2\rangle$(0.8155)
				$\|H-1\rightarrow L+1\rangle$(0.3002)
IV	$3B_{3u}^{+}$	8.73	0.281	$\|H-2\rightarrow L+3\rangle$−c.c.(0.4965)
				$\|H\rightarrow L+4\rangle$−c.c.(0.2280)
				$\|H\rightarrow L+1;H-1\rightarrow L+2\rangle$−c.c.(0.2260)

TABLE IV. Excited states contributing to the linear absorption spectrum of naphthalene computed using the FCI method coupled with the screened parameters in the PPP model Hamiltonian. The table includes many-particle wave functions, excitation energies, and dipole matrix elements of various states with respect to the ground state. DF corresponds to the dipole-forbidden state. "+c.c." indicates that the coefficient of the charge conjugate of a given configuration has the same sign, while "−c.c." implies that the two coefficients have opposite signs.

Peak	State	E (eV)	Transition dipole (Å)	Wave functions
DF	$1B_{3u}^{-}$	3.22	0.000	$\|H\rightarrow L+1\rangle$−c.c.(0.5965)
				$\|H\rightarrow L+1;H-3\rightarrow L\rangle$+c.c.(0.1564)
I	$1B_{2u}^{+}$	4.51	0.719	$\|H\rightarrow L\rangle$(0.9145)
II	$1B_{3u}^{+}$	5.30	1.640	$\|H\rightarrow L+1\rangle$+c.c.(0.6466)
III	$2B_{2u}^{+}$	6.12	0.842	$\|H-1\rightarrow L+1\rangle$(0.9012)
				$\|H\rightarrow L+1;H-1\rightarrow L+3\rangle$−c.c.(0.1334)
IV	$3B_{2u}^{+}$	7.52	0.844	$\|H-2\rightarrow L+2\rangle$(0.8496)

Anthraceme

TABLE V. Excited states contributing to the linear absorption spectrum of anthracene computed using the FCI method coupled with the standard parameters in the PPP model Hamiltonian. The table includes many-particle wave functions, excitation energies, and dipole matrix elements of various states with respect to the ground state. DF corresponds to the dipole-forbidden state. "+c.c." indicates that the coefficient of the charge conjugate of a given configuration has the same sign, while "−c.c." implies that the two coefficients have opposite signs.

Peak	State	E (eV)	Transition dipole (Å)	Wave functions
DF	$1B_{3u}^{-}$	3.25	0.000	$\|H\rightarrow L+1\rangle$−c.c.(0.5963)
				$\|H\rightarrow L+1;H-3\rightarrow L\rangle$−c.c.(0.1329)
				$\|H-2\rightarrow L+3\rangle$+c.c.(0.1268)
I	$1B_{2u}^{+}$	3.66	0.728	$\|H\rightarrow L\rangle$(0.8894)
				$\|H-1\rightarrow L+1\rangle$(0.2097)
II	$1B_{3u}^{+}$	5.34	2.040	$\|H\rightarrow L+1\rangle$+c.c.(0.6296)
III	$4B_{2u}^{+}$	6.94	1.069	$\|H-2\rightarrow L+2\rangle$(0.6612)
				$\|H-1\rightarrow L+1\rangle$(0.4093)
IV	$3B_{3u}^{+}$	7.70	0.436	$\|H-2\rightarrow L+3\rangle$−c.c.(0.4831)
				$\|H\rightarrow L;H\rightarrow L+2\rangle$−c.c.(0.2403)
V	$7B_{2u}^{+}$	8.30	0.769	$\|H-4\rightarrow L+4\rangle$(0.6955)
				$\|H-1\rightarrow L+5\rangle$+c.c.(0.2120)

TABLE VI. Excited states contributing to the linear absorption spectrum of anthracene computed using the FCI method coupled with the screened parameters in the PPP model Hamiltonian. The table includes many-particle wave functions, excitation energies, and dipole matrix elements of various states with respect to the ground state. DF corresponds to the dipole-forbidden state. "+c.c." indicates that the coefficient of the charge conjugate of a given configuration has the same sign, while "−c.c." implies that the two coefficients have opposite signs.

Peak	State	E (eV)	Transition dipole (Å)	Wave functions
DF	$1B_{3u}^{-}$	2.91	0.000	$\|H\rightarrow L+1\rangle$−c.c.(0.5670)
				$\|H\rightarrow L+1;H-3\rightarrow L\rangle$+c.c.(0.1500)
I	$1B_{2u}^{+}$	3.55	0.747	$\|H\rightarrow L\rangle$(0.8890)
II	$1B_{3u}^{+}$	4.64	2.019	$\|H\rightarrow L+1\rangle$+c.c.(0.6215)
III	$2B_{2u}^{+}$	5.93	0.613	$\|H-1\rightarrow L+1\rangle$(0.7680)
				$\|H\rightarrow L+4\rangle$−c.c.(0.2283)
	$3B_{2u}^{+}$	6.01	0.669	$\|H\rightarrow L+4\rangle$−c.c.(0.5024)
				$\|H-1\rightarrow L+1\rangle$(0.3616)
				$\|H-2\rightarrow L+2\rangle$(0.2987)
IV	$2B_{3u}^{+}$	6.63	0.519	$\|H\rightarrow L+5\rangle$+c.c.(0.3598)
				$\|H\rightarrow L;H\rightarrow L+2\rangle$+c.c.(0.3170)
				$\|H-2\rightarrow L+3\rangle$−c.c.(0.3161)
V	$7B_{2u}^{+}$	7.82	0.744	$\|H-4\rightarrow L+4\rangle$(0.5739)
				$\|H-3\rightarrow L+3\rangle$(0.3848)
				$\|H\rightarrow L;H-1\rightarrow L+2\rangle$−c.c.(0.2012)

Tetracene

TABLE VII. Excited states contributing to the linear absorption spectrum of tetracene computed using the QCI method for A_g and B_{2u} states and the MRSDCI method for B_{3u} states coupled with the standard parameters in the PPP model Hamiltonian. The table includes many-particle wave functions, excitation energies, and dipole matrix elements of various states with respect to the ground state. DF corresponds to the dipole-forbidden state. "+c.c." indicates that the coefficient of the charge conjugate of a given configuration has the same sign, while "−c.c." implies that the two coefficients have opposite signs.

Peak	State	E (eV)	Transition dipole (Å)	Wave functions
DF	$1B_{3u}^-$	3.22	0.000	$\|H\rightarrow L+2\rangle$−c.c.(0.5887)
				$\|H-1\rightarrow L+4\rangle$+c.c.(0.1395)
				$\|H\rightarrow L+2;H-4\rightarrow L\rangle$−c.c.(0.1289)
I	$1B_{2u}^+$	3.16	0.806	$\|H\rightarrow L\rangle$(0.8761)
II	$1B_{3u}^+$	5.15	2.392	$\|H\rightarrow L+2\rangle$+c.c.(0.6198)
III	$4B_{2u}^+$	6.35	0.799	$\|H-2\rightarrow L+2\rangle$(0.5623)
				$\|H-1\rightarrow L+1\rangle$(0.4056)
				$\|H-3\rightarrow L+3\rangle$(0.2211)
				$\|H-1\rightarrow L+5\rangle$+c.c.(0.2066)
IV	$9B_{2u}^+$	7.90	0.939	$\|H-3\rightarrow L+3\rangle$(0.4981)
				$\|H-2\rightarrow L+6\rangle$−c.c.(0.2665)
				$\|H-2\rightarrow L+2\rangle$(0.1925)
				$\|H-5\rightarrow L+5\rangle$(0.1921)
				$\|H-4\rightarrow L+4\rangle$(0.1879)

TABLE VIII. Excited states contributing to the linear absorption spectrum of tetracene computed using the QCI method for A_g and B_{2u} states and the MRSDCI method for B_{3u} states coupled with the screened parameters in the PPP model Hamiltonian. The table includes many-particle wave functions, excitation energies, and dipole matrix elements of various states with respect to the ground state. DF corresponds to the dipole-forbidden state. "+c.c." indicates that the coefficient of the charge conjugate of a given configuration has the same sign, while "−c.c." implies that the two coefficients have opposite signs.

Peak	State	E (eV)	Transition dipole (Å)	Wave functions
DF	$1B_{3u}^-$	3.02	0.000	$\|H\rightarrow L+2\rangle$−c.c.(0.5750)
				$\|H-2\rightarrow L;H\rightarrow L+4\rangle$−c.c.(0.1552)
I	$1B_{2u}^+$	2.97	0.799	$\|H\rightarrow L\rangle$(0.8683)
II	$1B_{3u}^+$	4.68	2.356	$\|H\rightarrow L+2\rangle$+c.c.(0.6269)
III	$3B_{2u}^+$	5.41	0.671	$\|H-1\rightarrow L+1\rangle$(0.7657)
				$\|H\rightarrow L+3\rangle$−c.c.(0.2076)
IV	$2B_{3u}^+$	6.03	0.573	$\|H\rightarrow L;H\rightarrow L+1\rangle$+c.c.(0.4998)
				$\|H-4\rightarrow L+1\rangle$+c.c.(0.2119)
				$\|H-1\rightarrow L+1;H\rightarrow L+1\rangle$+c.c.(0.2004)
	$4B_{2u}^+$	6.10	0.841	$\|H-2\rightarrow L+2\rangle$(0.7957)
V	$5B_{3u}^+$	7.22	0.413	$\|H-3\rightarrow L+2\rangle$−c.c.(0.3768)
				$\|H\rightarrow L;H\rightarrow L+1\rangle$−c.c.(0.2426)
				$\|H\rightarrow L;H\rightarrow L+5\rangle$+c.c.(0.2345)
				$\|H-1\rightarrow L+4\rangle$+c.c.(0.2177)
	$9B_{2u}^+$	7.37	0.901	$\|H-3\rightarrow L+3\rangle$(0.7722)
VI	$16B_{2u}^+$	8.44	0.650	$\|H-5\rightarrow L+5\rangle$(0.6119)
				$\|H\rightarrow L+1;H-4\rightarrow L+1\rangle$+c.c.(0.1790)

Pentacene

TABLE IX. Excited states contributing to the linear absorption spectrum of pentacene computed using the QCI method for A_g and B_{2u} states and the MRSDCI method for B_{3u} states coupled with the standard parameters in the PPP model Hamiltonian. The table includes many-particle wave functions, excitation energies, and dipole matrix elements of various states with respect to the ground state. DF corresponds to the dipole-forbidden state. "+c.c." indicates that the coefficient of the charge conjugate of a given configuration has the same sign, while "−c.c." implies that the two coefficients have opposite signs.

Peak	State	E (eV)	Transition dipole (Å)	Wave functions
DF	$1B_{3u}^{-}$	3.17	0.000	$\|H\rightarrow L+2\rangle$+c.c.(0.5519)
				$\|H\rightarrow L;H\rightarrow L+1\rangle$+c.c.(0.1439)
				$\|H-1\rightarrow L+4\rangle$+c.c.(0.1341)
I	$1B_{2u}^{+}$	2.86	0.838	$\|H\rightarrow L\rangle$(0.8568)
II	$1B_{3u}^{+}$	5.01	2.721	$\|H\rightarrow L+2\rangle$−c.c.(0.5950)
				$\|H-1\rightarrow L+4\rangle$−c.c.(0.1467)
	$3B_{2u}^{+}$	5.16	0.432	$\|H-1\rightarrow L+1\rangle$(0.5108)
				$\|H\rightarrow L+3\rangle$+c.c.(0.3155)
				$\|H-2\rightarrow L+2\rangle$(0.2668)
III	$4B_{3u}^{+}$	7.09	0.462	$\|H-1\rightarrow L+4\rangle$−c.c.(0.3674)
				$\|H\rightarrow L;H\rightarrow L+5\rangle$+c.c.(0.2329)
				$\|H\rightarrow L;H\rightarrow L+1\rangle$−c.c.(0.1848)
	$5B_{3u}^{+}$	7.23	0.413	$\|H-1\rightarrow L+1;H\rightarrow L+1\rangle$−c.c.(0.2762)
				$\|H\rightarrow L;H-1\rightarrow L+3\rangle$−c.c.(0.2266)
				$\|H\rightarrow L+7\rangle$+c.c.(0.2263)
	$11B_{2u}^{+}$	7.27	0.668	$\|H-3\rightarrow L+3\rangle$(0.4121)
				$\|H-6\rightarrow L+3\rangle$+c.c.(0.2475)
				$\|H-4\rightarrow L+4\rangle$(0.2374)
IV	$12B_{2u}^{+}$	7.58	0.672	$\|H-3\rightarrow L+3\rangle$(0.3294)
				$\|H-2\rightarrow L+2\rangle$(0.2682)
				$\|H-5\rightarrow L+5\rangle$(0.2125)
				$\|H-1\rightarrow L+5\rangle$−c.c.(0.2060)
	$6B_{3u}^{+}$	7.60	0.495	$\|H-3\rightarrow L+2\rangle$−c.c.(0.3907)
				$\|H-1\rightarrow L+4\rangle$−c.c.(0.2922)
				$\|H\rightarrow L;H\rightarrow L+1\rangle$−c.c.(0.2172)

TABLE X. Excited states contributing to the linear absorption spectrum of pentacene computed using the QCI method for A_g and B_{2u} states and the MRSDCI method for B_{3u} states coupled with the screened parameters in the PPP model Hamiltonian. The table includes many-particle wave functions, excitation energies, and dipole matrix elements of various states with respect to the ground state. DF corresponds to the dipole-forbidden state. "+c.c." indicates that the coefficient of the charge conjugate of a given configuration has the same sign, while "−c.c." implies that the two coefficients have opposite signs.

Peak	State	E (eV)	Transition dipole (Å)	Wave functions
DF	$1B_{3u}^{-}$	2.99	0.000	$\|H\rightarrow L+2\rangle$+c.c.(0.5117)
				$\|H\rightarrow L;H\rightarrow L+1\rangle$−c.c.(0.2348)
				$\|H\rightarrow L+2;H-4\rightarrow L\rangle$−c.c.(0.1394)
I	$1B_{2u}^{+}$	2.65	0.824	$\|H\rightarrow L\rangle$(0.8464)
II	$1B_{3u}^{+}$	4.65	2.642	$\|H\rightarrow L+2\rangle$−c.c.(0.6146)
	$2B_{2u}^{+}$	4.63	0.317	$\|H\rightarrow L+3\rangle$+c.c.(0.5123)
				$\|H\rightarrow L\rangle$(0.3994)
III	$4B_{3u}^{+}$	6.47	0.593	$\|H-4\rightarrow L+1\rangle$−c.c.(0.4034)
				$\|H-1\rightarrow L+1;H\rightarrow L+1\rangle$+c.c.(0.2226)
				$\|H\rightarrow L;H-1\rightarrow L+3\rangle$−c.c.(0.2216)
IV	$11B_{2u}^{+}$	6.77	0.782	$\|H-3\rightarrow L+3\rangle$(0.7460)
				$\|H\rightarrow L;H\rightarrow L;H-3\rightarrow L+3\rangle$(0.2030)
				$\|H\rightarrow L+6\rangle$−c.c.(0.1413)

Hexacene

TABLE XI. Excited states contributing to the linear absorption spectrum of hexacene computed using the MRSDCI method coupled with the standard parameters in the PPP model Hamiltonian. The table includes many-particle wave functions, excitation energies, and dipole matrix elements of various states with respect to the ground state. DF corresponds to the dipole-forbidden state. "+c.c." indicates that the coefficient of the charge conjugate of a given configuration has the same sign, while "−c.c." implies that the two coefficients have opposite signs.

Peak	State	E (eV)	Transition dipole (Å)	Wave functions
DF	$1B_{3u}^{-}$	3.07	0.000	$\|H\rightarrow L;H\rightarrow L+1\rangle$+c.c.(0.4407)
				$\|H\rightarrow L+3\rangle$+c.c.(0.2729)
				$\|H\rightarrow L+7\rangle$+c.c.(0.1758)
I	$1B_{2u}^{+}$	2.71	0.812	$\|H\rightarrow L\rangle$(0.8584)
II	$2B_{2u}^{+}$	4.19	0.733	$\|H\rightarrow L+2\rangle$+c.c.(0.5045)
				$\|H\rightarrow L;H-1\rightarrow L+3\rangle$+c.c.(0.1810)
				$\|H\rightarrow L;H\rightarrow L+4\rangle$−c.c.(0.1720)
III	$1B_{3u}^{+}$	4.61	3.049	$\|H\rightarrow L+3\rangle$−c.c.(0.5550)
				$\|H-4\rightarrow L+1\rangle$+c.c.(0.1653)
IV	$5B_{2u}^{+}$	5.87	0.764	$\|H\rightarrow L+6\rangle$+c.c.(0.4457)
				$\|H-1\rightarrow L+5\rangle$+c.c.(0.1821)
V	$4B_{3u}^{+}$	6.42	0.549	$\|H\rightarrow L;H\rightarrow L+1\rangle$+c.c.(0.3513)
				$\|H-1\rightarrow L+4\rangle$+c.c.(0.2390)
				$\|H-1\rightarrow L+1;H\rightarrow L+1\rangle$−c.c.(0.2092)
	$9B_{2u}^{+}$	6.51	0.619	$\|H-1\rightarrow L+5\rangle$+c.c.(0.2787)
				$\|H\rightarrow L+1;H\rightarrow L+3\rangle$+c.c.(0.2784)
VI	$11B_{2u}^{+}$	6.87	0.256	$\|H-3\rightarrow L+3\rangle$(0.4731)
				$\|H-1\rightarrow L+5\rangle$+c.c.(0.2414)
				$\|H-5\rightarrow L+5\rangle$(0.2177)
	$6B_{3u}^{+}$	6.90	0.478	$\|H\rightarrow L;H\rightarrow L+8\rangle$+c.c.(0.4054)
				$\|H\rightarrow L;H-1\rightarrow L+6\rangle$+c.c.(0.2608)
				$\|H\rightarrow L;H-2\rightarrow L+5\rangle$+c.c.(0.2090)
VI	$7B_{3u}^{+}$	7.01	0.585	$\|H-1\rightarrow L+4\rangle$+c.c.(0.3445)
				$\|H\rightarrow L;H-1\rightarrow L+2\rangle$+c.c.(0.2463)
				$\|H\rightarrow L;H\rightarrow L+8\rangle$+c.c.(0.2163)
				$\|H-2\rightarrow L+3\rangle$+c.c.(0.2019)

TABLE XII. Excited states contributing to the linear absorption spectrum of hexacene computed using the MRSDCI method coupled with the screened parameters in the PPP model Hamiltonian. The table includes many-particle wave functions, excitation energies, and dipole matrix elements of various states with respect to the ground state. DF corresponds to the dipole-forbidden state. "+c.c." indicates that the coefficient of the charge conjugate of a given configuration has the same sign, while "−c.c." implies that the two coefficients have opposite signs.

Peak	State	E (eV)	Transition dipole (Å)	Wave functions
DF	$1B_{3u}^{-}$	2.77	0.000	$\|H\rightarrow L;H\rightarrow L+1\rangle$+c.c.(0.4943)
				$\|H\rightarrow L+3\rangle$+c.c.(0.1830)
				$\|H-1\rightarrow L;H\rightarrow L+2\rangle$−c.c.(0.1819)
I	$1B_{2u}^{+}$	2.38	0.787	$\|H\rightarrow L\rangle$(0.8683)
II	$2B_{2u}^{+}$	3.94	0.716	$\|H-1\rightarrow L+1\rangle$(0.7077)
				$\|H\rightarrow L+2\rangle$−c.c.(0.3154)
	$1B_{3u}^{+}$	4.07	2.948	$\|H\rightarrow L+3\rangle$−c.c.(0.5956)
III	$6B_{2u}^{+}$	5.58	0.414	$\|H\rightarrow L+6\rangle$+c.c.(0.3583)
				$\|H-1\rightarrow L+5\rangle$−c.c.(0.3188)
				$\|H-2\rightarrow L+2\rangle$(0.2851)
	$4B_{3u}^{+}$	5.61	0.971	$\|H-1\rightarrow L+4\rangle$+c.c.(0.4188)
				$\|H\rightarrow L+7\rangle$−c.c.(0.2382)
				$\|H\rightarrow L;H-1\rightarrow L+2\rangle$+c.c.(0.2368)
				$\|H-1\rightarrow L+1;H\rightarrow L+1\rangle$−c.c.(0.2054)
IV	$9B_{2u}^{+}$	5.93	0.672	$\|H-2\rightarrow L+2\rangle$(0.6354)
				$\|H-1\rightarrow L+5\rangle$−c.c.(0.2745)
V	$8B_{3u}^{+}$	6.23	0.555	$\|H-2\rightarrow L+3\rangle$+c.c.(0.5539)
				$\|H\rightarrow L+7\rangle$−c.c.(0.1646)
				$\|H\rightarrow L;H-1\rightarrow L+2\rangle$+c.c.(0.1097)
VI	$18B_{2u}^{+}$	7.71	0.714	$\|H-3\rightarrow L+3\rangle$(0.6973)

Heptacene

TABLE XIII. Excited states contributing to the linear absorption spectrum of heptacene computed using the MRSDCI method coupled with the standard parameters in the PPP model Hamiltonian. The table includes many-particle wave functions, excitation energies, and dipole matrix elements of various states with respect to the ground state. DF corresponds to the dipole-forbidden state. "+c.c." indicates that the coefficient of the charge conjugate of a given configuration has the same sign, while "−c.c." implies that the two coefficients have opposite signs.

Peak	State	E (eV)	Transition dipole (Å)	Wave functions
DF	$1B_{3u}^{-}$	2.73	0.000	$\|H\rightarrow L;H\rightarrow L+1\rangle$+c.c.(0.4896)
				$\|H\rightarrow L+1;H-2\rightarrow L\rangle$+c.c.(0.1904)
				$\|H\rightarrow L+1;H\rightarrow L+2\rangle$+c.c.(0.1712)
I	$1B_{2u}^{+}$	2.63	0.793	$\|H\rightarrow L\rangle$(0.8563)
II	$1B_{3u}^{+}$	4.48	3.251	$\|H\rightarrow L+3\rangle$−c.c.(0.5033)
				$\|H\rightarrow L;H\rightarrow L+1\rangle$−c.c.(0.2170)
				$\|H-1\rightarrow L+5\rangle$+c.c.(0.1789)
III	$6B_{2u}^{+}$	5.96	0.326	$\|H\rightarrow L;H\rightarrow L+5\rangle$−c.c.(0.3368)
				$\|H\rightarrow L+1;H\rightarrow L+3\rangle$+c.c.(0.3312)
				$\|H-1\rightarrow L+1\rangle$(0.1997)
	$4B_{3u}^{+}$	6.01	0.490	$\|H\rightarrow L;H-1\rightarrow L+2\rangle$−c.c.(0.4204)
				$\|H-2\rightarrow L+2;H\rightarrow L+1\rangle$−c.c.(0.1781)
IV	$7B_{3u}^{+}$	6.70	0.624	$\|H-1\rightarrow L+5\rangle$+c.c.(0.3258)
				$\|H\rightarrow L;H-1\rightarrow L+2\rangle$−c.c.(0.2972)
				$\|H\rightarrow L;H\rightarrow L+4\rangle$+c.c.(0.2444)
V	$12B_{2u}^{+}$	7.09	0.736	$\|H-2\rightarrow L+2\rangle$(0.3457)
				$\|H-3\rightarrow L+3\rangle$(0.3312)

TABLE XIV. Excited states contributing to the linear absorption spectrum of heptacene computed using the MRSDCI method coupled with the screened parameters in the PPP model Hamiltonian. The table includes many-particle wave functions, excitation energies, and dipole matrix elements of various states with respect to the ground state. DF corresponds to the dipole-forbidden state. "+c.c." indicates that the coefficient of the charge conjugate of a given configuration has the same sign, while "–c.c." implies that the two coefficients have opposite signs.

Peak	State	E (eV)	Transition dipole (Å)	Wave functions
DF	$1B_{3u}^{-}$	2.35	0.000	$\|H\rightarrow L;H\rightarrow L+1\rangle$+c.c.(0.5062)
				$\|H-1\rightarrow L;H\rightarrow L+2\rangle$+c.c.(0.1942)
				$\|H\rightarrow L+1;H\rightarrow L+2\rangle$+c.c.(0.1648)
I	$1B_{2u}^{+}$	2.24	0.795	$\|H\rightarrow L\rangle$(0.8675)
II	$1B_{3u}^{+}$	3.80	1.900	$\|H\rightarrow L;H\rightarrow L+1\rangle$–c.c.(0.4795)
				$\|H-1\rightarrow L+1;H\rightarrow L+1\rangle$–c.c.(0.2362)
				$\|H\rightarrow L+3\rangle$–c.c.(0.1781)
	$3B_{2u}^{+}$	3.87	0.459	$\|H\rightarrow L+2\rangle$+c.c.(0.5254)
				$\|H-1\rightarrow L+1\rangle$(0.4140)
	$2B_{3u}^{+}$	3.98	2.553	$\|H\rightarrow L+3\rangle$–c.c.(0.5710)
III	$4B_{2u}^{+}$	4.92	0.459	$\|H-2\rightarrow L+2\rangle$+(0.4342)
				$\|H-1\rightarrow L+4\rangle$+c.c.(0.4189)
				$\|H\rightarrow L+6\rangle$+c.c.(0.2618)
	$4B_{3u}^{+}$	4.98	0.799	$\|H\rightarrow L;H-1\rightarrow L+2\rangle$–c.c.(0.4219)
IV	$5B_{3u}^{+}$	5.34	0.668	$\|H\rightarrow L+7\rangle$–c.c.(0.4384)
				$\|H\rightarrow L;H-1\rightarrow L+2\rangle$–c.c.(0.2542)
	$7B_{2u}^{+}$	5.36	0.609	$\|H-2\rightarrow L+2\rangle$(0.5520)
				$\|H-1\rightarrow L+4\rangle$+c.c.(0.3475)
V	$7B_{3u}^{+}$	5.57	0.867	$\|H-1\rightarrow L+5\rangle$+c.c.(0.4741)
				$\|H\rightarrow L+7\rangle$–c.c.(0.2927)
				$\|H\rightarrow L;H-1\rightarrow L+2\rangle$–c.c.(0.1582)
VI	$20B_{2u}^{+}$	8.39	0.871	$\|H-4\rightarrow L+4\rangle$(0.7058)

*Electronic address: psony@phy.iitb.ac.in
†Electronic address: shukla@phy.iitb.ac.in

[1] D. J. Gundlach, Y. Y. Lin, T. N. Jackson, S. F. Nelson, and D. G. Schlom, IEEE Electron Device Lett. **18**, 87 (1997).
[2] S. F. Nelson, Y. Y. Lin, D. J. Gundlach, and T. N. Jackson, Appl. Phys. Lett. **72**, 1854 (1998).
[3] V. Y. Butko, X. Chi, D. V. Lang, and A. P. Ramirez, Appl. Phys. Lett. **83**, 4773 (2003).
[4] K. Tanabe, K. Ohzeki, S. Nankai, and T. Yamabe, J. Phys. Chem. **41**, 1069 (1983).
[5] S. Kivelson and O. L. Chapman, Phys. Rev. B **28**, 7236 (1983).
[6] A. Hepp, H. Heil, W. Weise, M. Ahles, R. Schmechel, and H. von Seggern, Phys. Rev. Lett. **91**, 157406 (2003).
[7] K. Hummer, P. Puschnig, and C. Ambrosch-Draxl, Phys. Rev. B **67**, 184105 (2003).
[8] K. Hummer and C. Ambrosch-Draxl, Phys. Rev. B **71**, 081202(R) (2005).
[9] Y. C. Cheng, R. J. Silbey, D. A. da Silva Filho, J. P. Calbert, J. Cornil, and J. L. Brédas, J. Chem. Phys. **118**, 3764 (2003).
[10] See, e.g., E. Clar, *Polycyclic Hydrocarbons* (Academic Press, London, 1964).
[11] H. B. Klevens and J. R. Platt, J. Chem. Phys. **17**, 470 (1949).
[12] D. Biermann and W. Schmidt, J. Am. Chem. Soc. **102**, 3163 (1980).
[13] J. B. Birks, L. G. Christophorou, and R. H. Huebner, Nature (London) **217**, 809 (1968).
[14] D. Bebelaar, Chem. Phys. **3**, 205 (1974).
[15] A. Bergman and J. Jortner, Chem. Phys. Lett. **26**, 323 (1974).
[16] R. H. Huebner, S. R. Mielczarek, and C. E. Kuyatt, Chem. Phys. Lett. **16**, 464 (1972).
[17] A. S. Aleksandrovsky, S. V. Karpov, S. A. Myslivets, A. K. Popov, and V. V. Slabko, J. Phys. B **26**, 2965 (1993).
[18] N. Mikami and M. Ito, Chem. Phys. Lett. **31**, 472 (1975).
[19] B. Dick and G. Hohlneicher, Chem. Phys. Lett. **84**, 471 (1981).
[20] A. Bergman and J. Jortner, Chem. Phys. Lett. **15**, 309 (1972).
[21] R. P. Steiner and J. Michl, J. Am. Chem. Soc. **100**, 6861 (1978).
[22] W. R. Lambert, P. M. Felker, J. A. Syage, and A. H. Zewail, J. Chem. Phys. **81**, 2195 (1984).
[23] B. Dick and G. Hohlneicher, Chem. Phys. Lett. **83**, 615 (1981).
[24] L. E. Lyons and G. C. Morris, J. Mol. Spectrosc. **4**, 480 (1960).
[25] K. F. Man, S. Trajmar, J. W. McConkey, J. M. Ratliff and M. Khakoo, J. Phys. B **25**, 5245 (1992).
[26] L. Sebastian, G. Weiser, G. Peter, and H. Bässler, Chem. Phys. **75**, 103 (1983).
[27] J. Wolf and G. Holhneicher, Chem. Phys. **181**, 185 (1994).
[28] E. Sackmann and H. Wöhwald, J. Chem. Phys. **58**, 5407 (1973).
[29] L. Sebastian, G. Weiser, and H. Bässler, Chem. Phys. **61**, 125 (1981).

[30] I. B. Berlman, *Handbook of Fluorescence Spectra of Aromatic Molecules*, 2nd ed. (Academic Press, New York, 1971).
[31] A. Bree and L. E. Lyons, J. Chem. Soc. **1960**, 5206.
[32] J. B. Birks, *Photophysics of Aromatic Molecules* (Wiley-Interscience, New York, 1970).
[33] P. D. Burrow, J. A. Michejda, and K. D. Jordan, J. Chem. Phys. **86**, 9 (1987).
[34] S. C. Dahlberg and M. E. Musser, J. Chem. Phys. **71**, 2806 (1979).
[35] E. Heinecke, D. Hartmann, R. Müller, and A. Hese, J. Chem. Phys. **109**, 906 (1998).
[36] T. M. Halasinski, D. M. Hudgins, F. Salama, L. J. Alamandola, and T. Bally, J. Phys. Chem. A **104**, 7484 (2000).
[37] S. P. Park, S. S. Kim, J. H. Kim, C. N. Whang, and S. Im, Appl. Phys. Lett. **80**, 2872 (2002).
[38] S. S. Kim, S. P. Park, J. H. Kim, and S. Im, Thin Solid Films **420-421**, 19 (2002).
[39] J. Puigdollers, C. Voz, A. Orpella, I. Martin, M. Vetter, and R. Alcubilla, Thin Solid Films **427**, 367 (2003).
[40] R. He, I. Dujovne, L. Chen, Q. Miao, C. F. Hirjibehedin, A. Pinczuk, C. Nuckolls, C. Kloc, and A. Ron, Appl. Phys. Lett. **84**, 987 (2004).
[41] J. Lee, S. S. Kim, K. Kim, J. H. Kim, and S. Im, Appl. Phys. Lett. **84**, 1701 (2004).
[42] H. Angliker, E. Rommel, and J. Wirz, Chem. Phys. Lett. **87**, 208 (1982).
[43] C. A. Coulson, Proc. Phys. Soc. London **60**, 257 (1948).
[44] J. Pariser, J. Chem. Phys. **24**, 250 (1956).
[45] J. R. Platt, J. Chem. Phys. **17**, 484 (1949).
[46] N. S. Ham and K. Ruedenberg, J. Chem. Phys. **25**, 13 (1956).
[47] O. C. Hofer and R. M. Hedges, Chem. Phys. Lett. **6**, 67 (1970).
[48] Y. Kawashima, T. Hashimoto, H. Nakano, and K. Hirao, Theor. Chem. Acc. **102**, 49 (1999).
[49] C. Raghu, Y. Anusooya Pati, and S. Ramasesha, Phys. Rev. B **65**, 155204 (2002).
[50] C. Raghu, Y. Anusooya Pati, and S. Ramasesha, Phys. Rev. B **66**, 035116 (2002).
[51] E. S. Kadantsev, M. J. Stott, and Angel Rubio, J. Chem. Phys. **124**, 134901 (2006).
[52] S. Grimme and M. Parac, Tech. Rep. Ser. - I. A. E. A. **4**, 292 (2003).
[53] K. B. Wiberg, J. Org. Chem. **62**, 5720 (1997).
[54] H. H. Heinze, A. Görling, and N. Rösch, J. Chem. Phys. **113**, 2088 (2000).
[55] K. N. Houk, S. L. Patrick, and M. Nendel, J. Org. Chem. **66**, 5517 (2001).
[56] M. Baldo, A. Grassi, R. Pucci, and P. Tomasello, J. Chem. Phys. **77**, 2438 (1982).
[57] N. O. Lipari and C. B. Duke, J. Chem. Phys. **63**, 1768 (1975).
[58] See, e.g., D. Barieswyl, D. K. Campbell, and S. Mazumdar, in *Conjugated Conducting Polymers*, edited by H. Keiss (Springer-Verlag, Berlin, 1992), pp. 7–133.
[59] H. Ghosh, A. Shukla, and S. Mazumdar, Phys. Rev. B **62**, 12763 (2000).
[60] A. Shukla, Phys. Rev. B **65**, 125204 (2002).
[61] A. Shukla, H. Ghosh, and S. Mazumdar, Phys. Rev. B **67**, 245203 (2003).
[62] A. Shukla, Chem. Phys. **300**, 177 (2004).
[63] A. Shukla, Phys. Rev. B **69**, 165218 (2004).
[64] P. Sony and A. Shukla, Phys. Rev. B **71**, 165204 (2005).
[65] K. Ohno, Theor. Chim. Acta **2**, 219 (1964).
[66] M. Chandross and S. Mazumdar, Phys. Rev. B **55**, 1497 (1997).
[67] See, e.g., R. B. Campbell and J. M. Robertson, Acta Crystallogr. **15**, 289 (1962).
[68] M. Dierksen and S. Grimme, J. Chem. Phys. **120**, 3544 (2004).
[69] M. S. Deleuze, L. Claes, E. S. Kryachko, and J.-P. Francois, J. Chem. Phys. **119**, 3106 (2003).
[70] J. Cioslowski, J. Chem. Phys. **98**, 473 (1993).
[71] M. A. Garcia-Bach, A. Peñaranda, and D. J. Klein, Phys. Rev. B **45**, 10891 (1992).
[72] T. A. Niehaus, M. Rohlfing, F. Della Sala, A. DiCarlo, and Th. Frauenheim, Phys. Rev. A **71**, 022508 (2005).
[73] S. Ramasesha and Z. G. Soos, Chem. Phys. **91**, 35 (1984).
[74] S. Ramasesha, D. S. Galvao, and Z. G. Soos, J. Phys. Chem. **97**, 2823 (1993).
[75] P. Sony and A. Shukla, Synth. Met. **155**, 316 (2005).
[76] P. Tavan and K. Schulten, J. Chem. Phys. **70**, 5414 (1979).
[77] H. E. Simmons, J. Chem. Phys. **40**, 3554 (1964).
[78] H. Nakatsuji, M. Komori, and O. Kitao, Chem. Phys. Lett. **142**, 446 (1987).
[79] T. Hashimoto, H. Nakano, and K. Hirao, J. Chem. Phys. **104**, 6244 (1996).
[80] J. L. Brédas and G. B. Street, J. Phys. C **18**, L651 (1985).
[81] R. A. Street, D. Knipp, and A. R. Völkel, Appl. Phys. Lett. **80**, 1658 (2002).
[82] H. Klauk, D. J. Gundlach, J. A. Nichols, and T. N. Jackson, IEEE Trans. Electron Devices **46**, 1258 (1999).
[83] H. Klauk, D. J. Gundlach, and T. N. Jackson, IEEE Electron Device Lett. **20**, 289 (1999).
[84] M. L. Tiago, J. E. Northrup, and S. G. Louie, Phys. Rev. B **67**, 115212 (2003).
[85] E. Clar, *Polycyclic Hydrocarbons* (Academic Press, London, 1964) Vol. 1, p. 2; *The Aromatic Sextet* (Wiley, London, 1972); edited by A. Bjorseth, *Handbook of Polycyclic Aromatic Hydrocarbons* (Dekker, New York, 1983); *Polynuclear Aromatic Hydrocarbons: A Decade of Progress*, editor by M. Cooke and A. J. Dennis, (Battelle Press, Columbus 1988); , D. Biermann and W. J. Schmidt, J. Am. Chem. Soc. **102**, 8163 (1980); R. G. Harvey, *Polycyclic Aromatic Hydrocarbons* (Wiley-VCH, New York, 1997).
[86] J.-I. Aihara, Phys. Chem. Chem. Phys. **1**, 3193 (1999); , J. Phys. Chem. A **103**, 7487 (1999); , J. Am. Chem. Soc. **99**, 2048 (1977).
[87] J. Sauer and R. Sustmann, Angew. Chem., Int. Ed. Engl. **18**, 779 (1980); I. Fleming, *Frontier Orbital and Organic Chemical Reactions* (Wiley, Chichester 1976).
[88] W. E. Bachmann and L. B. Scott, J. Am. Chem. Soc. **70**, 1458 (1948); U. Girreser, D. Giuffrida, F. H. Kohnke, J. P. Mathias, D. Philip, and J. F. Stoddart, Pure Appl. Chem. **65**, 119 (1993); Y. Muruta, N. Kato, K. Fujiwara, and K. Komatsu, J. Org. Chem. **64**, 3483 (1999).
[89] W. C. Herndon and Jr. M. L. Ellzey, J. Am. Chem. Soc. **96**, 6631 (1974); W. C. Herndon, J. Chem. Soc., Chem. Commun. **1977**, 817.
[90] D. Z. Wang and A. Streitwieser, Theor. Chim. Acta **102**, 78 (1999).
[91] E. Clar, Chem. Ber. **72B**, 2137 (1939); C. Marschalk, Bull. Soc. Chim. Belg. **6**, 1112 (1939).
[92] Q. Xu, H. M. Duong, F. Wudl, and Y. Yang, Appl. Phys. Lett. **85**, 3357 (2004).

[93] M. Bendikov, F. Wudl, and D. F. Perepichka, Chem. Rev. (Washington, D.C.) **104**, 4891 (2004).
[94] E. Clar, Chem. Ber. **75B**, 1330 (1942).
[95] See also C. Marschalk, Bull. Soc. Chim. Belg. **10**, 511 (1943).
[96] W. J. Bailey and C.-W. Liaio, J. Am. Chem. Soc. **77**, 992 (1955).
[97] B. Boggiano and E. Clar, J. Chem. Soc. **1957**, 2681.
[98] R. Notario and J.-L. M. Abbound, J. Phys. Chem. A **102**, 5290 (1998).